THE USE OF IRON MATERIALS TO IMMOBILIZE RHENIUM, A CHEMICAL ANALOGUE FOR TECHNETIUM, IN CONTAMINATED WATER

by

ROBERT JAMES THOMAS

(Under the Direction of John C. Seaman)

ABSTRACT

Technetium ($^{99}Tc$), produced by nuclear fission of $^{235}U$ and $^{239}Pu$, is a long-term risk associated with radioactive liquid waste at U.S. Department of Energy sites. This study focused on remediating $^{99}Tc$ using rhenium (Re) as a chemical analogue to avoid working with potentially dangerous radionuclides. Batch experiments were performed to assess the ability of four commercially available Fe-based materials (porous iron composite, PIC, reagent grade zero valent iron, and two Fe oxides) to immobilize Re in the presence and absence of $NO_3^-$ and in oxic and anoxic environments. The PIC material was the most effective at immobilizing Re and reducing $NO_3^-$ under all treatment conditions. Column experiments were carried out as well to assess the effectiveness of the PIC material under kinetically limited conditions that are analogous to a permeable reactive barrier (PRB). The PIC material immobilized Re in the absence of $NO_3^-$. When $NO_3^-$ was present, Re breakthrough occurred much earlier.

INDEX WORDS: Rhenium, Iron materials, Sorption, Batch, Column, Zero-Valent Iron, Batch, Column

# THE USE OF IRON MATERIALS TO IMMOBILIZE RHENIUM, A CHEMICAL ANALOGUE FOR TECHNETIUM, IN CONTAMINATED WATER

by

ROBERT JAMES THOMAS

A.S., Waycross College, 2010

B.S., The University of Georgia, 2014

A Thesis Submitted to the Graduate Faculty of The University of Georgia in Partial Fulfillment of the Requirements for the Degree

MASTER OF SCIENCE

ATHENS, GEORGIA

2018

# THE USE OF IRON MATERIALS TO IMMOBILIZE RHENIUM, A CHEMICAL ANALOGUE FOR TECHNETIUM, IN CONTAMINATED WATER

by

ROBERT JAMES THOMAS

| | |
|---|---|
| Major Professor: | John C. Seaman |
| Committee: | Miguel L. Cabrera |
| | Aaron Thompson |
| | Fanny M. Coutelot |

Electronic Version Approved:

Suzanne Barbour
Dean of the Graduate School
The University of Georgia
December 2018

For my Mom, who taught me to be curious about my surroundings, who encouraged me and sacrificed for me so I could have a great education. For my Dad, who always believed in me and pushed me to keep going. Without their love, support and strength, I would not be where I am today.

## ACKNOWLEDGEMENTS

I would like to thank Drs. John Seaman, Fanny Coutelot, Miguel Cabrera, and Aaron Thompson for their guidance and support during my graduate studies at The University of Georgia. Special thanks is given to Dr. John Seaman and Dr. Fanny Coutelot for their encouragement and editing skills that helped greatly in my writing approach. Additional appreciation is given to Mrs. Angela Lindell for her analytical support in the lab. Special thanks is given to Dr. Dorcas Franklin for her encouragement to follow my interest and apply to graduate school, without her I would not have started this journey. I would also like to thank Matthew Baker, Kimberly Price, Emily Dorward, Jarad Cochran, and Liyun Zhang for their support in the lab.

Finally, I would like to thank Anthony Milligan for his continued support and encouragement throughout the last few years.

This research is supported through a Cooperative Agreement (DEFC09-07-SR22506) between the Department of Energy and The University of Georgia Research Foundation.

TABLE OF CONTENTS

Page

LIST OF TABLES

Page

LIST OF FIGURES

Page

# CHAPTER 1

# INTRODUCTION

When contaminants enter the subsurface environment, they become subject to a variety of complex physical, chemical, and biological processes. The design of an effective soil or groundwater remediation strategy requires a thorough understanding of such complex processes. This chapter provides a brief introduction to the chemical and physical processes that control the fate and transport of contaminants in the subsurface environment, with a special focus on the properties of the radiological contaminant Technetium (Tc) and its chemical surrogate Rhenium (Re). This is done in an effort to identify and develop potentially effective cleanup strategies.

## 1.1 Subsurface environment

### 1.1.1 Subsurface waters

The hydrologic cycle plays an important role in soil formation as well as the supply and quality of groundwater. The cycle begins with the evaporation of water from the earth's surface. As the water vapor rises it cools and condenses, forming clouds that are transported until it returns to earth's surface as precipitation. Once it hits the surface, it can be evaporated back to the atmosphere or penetrate the surface and recharges the groundwater (Figure 1.1).

Recharge can be generally defined as a downward flow of water reaching the water table (De Vries and Simmers, 2002). Subsurface water can be broken up into two zones: the unsaturated zone and saturated zone (groundwater, Figure 1.1). Water enters the soil in the unsaturated zone (vadose zone). In the vadose zone, three types of water exist (Figure 1.2). The first type is capillary water. Capillary water is water found in the micropores of soil, and is held against gravity by a combination of cohesion and adhesion (i.e., the attraction of water molecules to soil particles). This is the water that is available for plant uptake and is also known as the soil solution. The second type of water is gravitational water. Gravitational water is free water that moves through soil as a result of gravity. This water is found in the macropores in soil and moves rapidly through well drained soils after precipitation. The third type of water is hygroscopic water. Hygroscopic water forms very thin films around soil particles and is not available for plant uptake.

The capillary fringe is located directly above the water table (Figure 1.1). Here, capillary forces associated with small pores pulls groundwater up from the water table due to tension (Driscoll, 1986). Water located below the water table is known as groundwater, which is in the saturate zone. It is best to imagine groundwater as a large natural reservoir or system of reservoirs in rocks and soil whose capacity is the total volume of pores or openings that are filled with water.

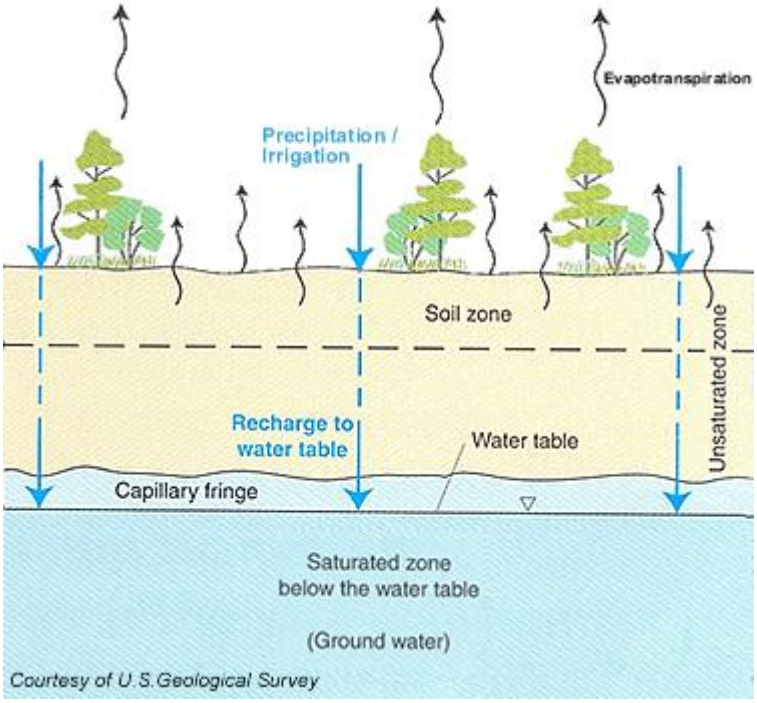


*Figure 1.1 Diagram showing the land surface through the vadose zone to the saturated zone*

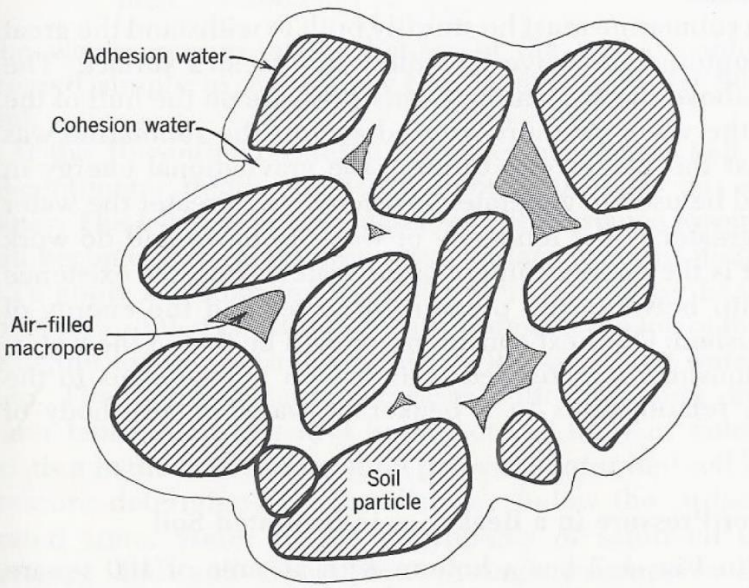


*Figure 1.2: Schematic showing the relationship of adhesion and cohesion water with respect to soil particles and air-filled macropores*

### 1.1.2 Water transport in subsurface environment

The retention and transport of water in the subsurface are energy-related phenomena (Boulding and Ginn, 1995). Free energy is the term used to describe the energy status of water. In general, water will move from an area of higher free energy to an area of lower free energy. The influence of the free energy of soil-water is described by three major types of energy potentials: 1) **Matric potential ($P_m$)** which is the attraction of water molecules to solids in the subsurface environment (Kazmann, 1988). This potential arises from both adsorption of water onto solids and capillary action in soil pores. In general, the smaller the particle and pore size, the greater the matric potential. 2) **Osmotic potential ($P_o$)** which results from solute ions attracting water molecules from areas of lower ion concentration to areas of higher ion concentrations (Marshall, 1959). 3) **Gravitational potential ($P_g$)** which is

the attraction of water towards the center of the earth due to gravitational forces (Te Chow, 1988). The total soil-water potential is the sum of the contributions of the various forces acting on soil water:

$$P_t = P_g + P_m + P_o + \cdots \qquad \text{Eq. 1.1}$$

where the gravitational, matric, and osmotic potentials are as defined above and other less significant potentials are indicated by dots. Matric and osmotic potentials are both negative potentials while gravitational potential is positive, thus water will only move through a soil profile if $P_g > P_m + P_o$. The driving force for water movement is the water potential gradient, which is the water potential difference between two points, divide by the distance between the two points (Foth, 1978).

In 1856, French engineer Henry Darcy, observed that the flow of water through the ground is the same as in a pipe. Using a pipe filled with saturated sand, Darcy demonstrated that the rate of flow is proportional to the difference in hydraulic head at the inlet and outlet of the column, and inversely proportional to the length of the column (Radcliffe and Šimůnek, 2010). The following equation is known as Darcy's Law:

$$J_w = -K_s \frac{\Delta H}{L} \qquad \text{Eq 1.2}$$

where $J_w$ is the volumetric flow rate of water per unit cross-sectional area, $K_s$ is the saturated hydraulic conductivity, $\Delta H$ is the change in hydraulic pressure head, and L is the length of the column. Darcy's Law is used to describe the movement of water in the saturated zone.

In 1931, American Soil Physicist Lorenzo Richards, formulated an equation that described vertical water movement under unsaturated conditions. The following equation is known as the Richards Equation:

$$\frac{\partial \theta}{\partial z} = \frac{\partial}{\partial z}\left[K(\theta)\left(\frac{\partial h}{\partial z} + 1\right)\right] \qquad \text{Eq 1.3}$$

where θ is the volumetric water content in a given unit area, *z* is the elevation head, *h* is the capillary pressure head, and *K* is the hydraulic conductivity. This is a non-linear partial differential equation. The left side of the equation is the rate of change of mass in a small control volume, resulting in this equation yielding water movement per unit (Hornberger et al., 2014).

There is an enormous number of organic and inorganic pollutants in the environment that reach the soil via dry/wet deposition or directly through anthropogenic applications. As water flows through the soil, chemicals may become sorbed, which retards their transport compared to the velocity of water. The fate of these pollutants depends upon the specific adsorption, degradation (for organics), and leaching processes to which they are subjected.

### 1.2 Metals/Trace Elements

A trace element (TEs) is an element found in natural materials (i.e., the lithosphere) at less than 0.1% of composition and when present at sufficient concentrations, may be toxic to living organisms. Some TEs are essential for the growth, development, and health of organisms (Cu, Co, Fe, Mn, Mo, Zn, Cr, F, Ni, Ni, Se, and Sn) (Underwood, 2012). However, the quantitative difference between essential amounts and biological excesses of

TEs are small. TEs can be metals, metalloids, or actinide elements that are derived from soil parent material, inputs to agricultural systems, industrial and municipal waste discharge, and nuclear waste (Adriano, 1986).

Trace elements are associated with different soil fractions and can exist in a variety of chemical forms or "species". The chemical speciation of a TE refers to the distribution amongst various potential species that can control environmental fate and transport. From the various origins of TEs, they may eventually reach the soil, their fate then depends on the chemical and physical properties of the soil and their speciation. TEs can adopt different forms when in soil solution. Trace elements undergo a series of reactions involving both the aqueous and solid phases which vary in time and space (Adriano, 2001a).

The mobility of TEs found in nature is determined by the stability of the host phase in relation to the particular weathering environment. Once the dissolution of the host mineral occurs, the TE is mobilized in the soil. The fate of it depends on the behavior of its aqueous chemical species, which can be related to such parameters as ionic potential and effective hydrated ionic diameter (Kabata-Pendias, 2010). The partitioning of TEs is a complex function of such environmental factors such as pH, Eh, $P_{CO2}$, the activity of ligand species, and also complicated by interactions with Organic Matter (OM) and colloidal material (Davies, 1980). Of these factors, the pH and Eh of the system are generally quite important.

The mobility of TEs in the soil designates the ability of it to pass from a form where it is retained with some energy into another where it is held with less energy (Juste, 1988). Therefore, TEs have the ability to pass through various forms where it is less and less energetically bonded leading into the soil solution. In the solid phase of soil, TEs can be absorbed or complexed on the surface of solid compounds. They can also be included in

either the crystal lattice or in an amorphous structure. The TEs are superficially adsorbed by solid components (i.e., clay minerals, iron (Fe), and manganese (Mn) oxides, or organic matter) are sorbed via several complex mechanisms, and may become more or less mobile with changes in the chemical environment. However, TEs structurally incorporated in soil minerals are far less susceptible to becoming mobile and may be slowly released over time as the minerals are progressively altered.

The physico-chemical processes at the solid-liquid interface that control TE partitioning include the following: ion exchange; surface complexation; precipitation and co-precipitation. The main soil constituents susceptible to TE sorption are phyllosilicate clays, carbonates, metal (hydr) oxides (mainly those from Fe and Mn), silicates, and organic matter. The main mechanisms influencing liquid-soil TE partitioning are:

- **Sorption**: sorption can be defined as the accumulation of a TE at an interface between the solid surface and soil solution. The term is more generally used to describe the loss of an element from the soil solution without implying the underlying mechanisms. If the sorption mechanism is based on valence forces, it is known as chemisorption, if the sorption mechanism is based on van der Waals' forces, then it is known as physisorption. The electrostatic forces involved in sorption can be explained by Coulomb's law of attraction between unlike charges and repulsion between like charges. At equilibrium, sorption by soil particles can be described by the Freundlich and Langmuir equations without implying a mechanism (Kinniburgh, 1986). In soil, the main components involved in sorption are hydrous oxides, organic matter, carbonates, and clay minerals (Adriano et al., 2004).

- **Complexation**: complexation refers to the overall chemical reaction occurring when a TE creates a stable entity with a surface functional group. There are two types of

surface complexes, outer-sphere and inner-sphere. These complexes can also occur on the edges of clay minerals. If a water molecule is present between the surface functional group and the bound TE, the surface complex is termed outer-sphere (Sposito, 1984). If there is no water molecule present between the TE and the surface functional group to which it is bound, this is an inner-sphere complex (Sparks, 2003).

- **Precipitation-dissolution**: the precipitation and dissolution processes are based on the equilibria of the soil solution. When oversaturation of a TE with respect to a solid phase occurs in the soil solution, the TE may precipitate as that phase. When the soil solution is undersaturated, dissolution of the solid phase may occur. However, the degree of saturation in no way implies the rate at which such a reaction may occur. Precipitation is then defined as the passage of a solute solution into a solid state depending on the equilibrium. Precipitation is the predominant process of metal immobilization in soils in the presence of anions such as sulfate, carbonate, hydroxide, and phosphate (Adriano, 2001b).

If a TE is present in the soil and groundwater at concentrations considered to be unsafe, it is considered to be a contaminant. When soil contamination occurs, it is important to understand the processes controlling the fate and transport of the contaminant in order to assess the risk associate with it, whether or not it will affect human population, and determine if a remedial action is necessary.

A common method of predicting TE partitionning is based on partition coefficient, $K_d$, values, equation 1.4, which is found by dividing the sorbed concentration of the TE by the concentration of the TE found in solution. Partitioning data is designed to investigate equilibrium processes. The $K_d$ value is a direct measure of the partitioning of a contaminant between the solid and aqueous phases (Leo et al., 1971). It is an experimental measurement

that attempts to account for various chemical and physical mechanisms that are influenced by numerous of variables.

$$K_d = \frac{[sorbed]}{[solution]} \qquad \text{Eq 1.4}$$

Values for $K_d$ vary between contaminants as well as a function of aqueous and solid phase chemistry (Delegard and Barney, 1983). For example, uranium $K_d$ values can vary over 6 orders of magnitude depending on the composition of the aqueous and solid phase chemistry (Kaplan and Serne, 1995). However, the $K_d$ is a fixed ratio for a very specific set of conditions; therefore, other characteristcs of the system are needed to better understand $K_d$ values. Ideally, when modeling TEs, values would be avaliable for a range of aqueous and geological conditions that reflect the system in question.

It is generally observed that as the concentration of a TE in solution increases, the amount of it sorbed to a solid surface also increases. A plot that describes the amount of a species sorbed as a function of its concentration in solution, measured at constant temperature, is known as a sorption isotherm (Langmuir, 1997). Sorption experiments are carried out by equilibrating (shaking or stirring) an adsorptive solution of a known composition with a known amount of adsorbent at a constant temperature and pressure for a period of time such that equilibrium is attained. After equilibrium is reached, the adsorptive solution is separated from the adsorbent by centrifugation, settling, or filtering, and then analyzed (Bleam, 2016). The pH and ionic strength are also controlled in most adsorption experiments. The degree of adsorption can be determined using the following mass balance equation:

$$\frac{(C_0V_0) - (C_fV_f)}{m} = q \qquad \text{Eq. 1.5}$$

where $q$ is the amount adsorbed (adsorbate per unit mass of adsorbent) in g $kg^{-1}$, $C_0$ and $C_f$ are the initial and final adsorbate concentrations, respectively in g $L^{-1}$, $V_0$ and $V_f$ are final adsorptive volumes, respectively in mL, and $m$ is the mass of the adsorbent in kg. Adsorption could then be described graphically by plotting $C_f$ or $C$ (where $C$ is referred to as equilibrium or final adsorptive concentration) on the x-axis versus $q$ on the y-axis (Sparks, 2013).

Equilibrium based models have been used to describe constituent adsorption on soil surfaces. The partition coefficient discussed above, i.e, Kd, is essentially a linear sorption isotherm, with the amount adsorbed directly related to the amount of adsorbate in solution. The two most common used non-linear sorption isotherms are the Freundlich and Langmuir equations. The Freundlich equation is purely empirical and shows decreasing sorption with increasing concentration as well as no apparent maximum and is expressed as:

$$S = K_F C^n \qquad \text{Eq. 1.6}$$

where $S$ is the amount sorbed in kg $g^{-1}$, $C$ is the amount remaining in solution in kg $mL^{-1}$, $K_F$ is the Freundlich partitioning coefficient in mL $kg^{-1}$, and $n$ is the exponential Freundlich term that is unit-less, and generally <1 (Appelo and Postma, 2004). At high concentrations of solute, the Freundlich model does not account for finite adsorption capacity; however, ignoring physical constraints when considering trace constituent adsorption is not usually critical.

The Langmuir equation describes decreasing sorption with increasing concentration up to a sorption maximum and is expressed as:

$$S = \frac{S_{max} K_L C}{1 + K_L C} \qquad \text{Eq. 1.7}$$

where $S_{max}$ is the maximum adsorption capacity of the solid per unit mass in kg $g^{-1}$ , $K_L$ is the Langmuir partitioning coefficient in mL $g^{-1}$, and $C$ is the concentration of the absorbate in kg $mL^{-1}$. The original assumptions of the Langmuir equation are (Harter and Smith, 1981): (1) Sorption occurs on planar surfaces that have a fixed number of sites that are identical and the sites can hold only one molecule, therefore only monolayer cover is permitted, which represents maximum sorption. (2) Sorption is reversible. (3) There is no lateral movement of molecules on the surface. (4) The sorption energy is the same for all sites and independent of surface coverage, and there is no interaction between the sorbate molecules. These assumptions are valid for ideal gases; however, they are not valid for the heterogeneous surfaces found in soils. Therefore the equation should only be used for purely qualitative and descriptive purposes (Langmuir, 1918).

### 1.3 Technetium

Technetium (Tc) is element 43 on the periodic table, and the lightest element (Z = 99) with no stable isotopes. The technetium-99 isotope ($^{99}$Tc) is a major fission product of $^{235}$U and $^{239}$Pu in nuclear reactors, with a high fission yield (ca. 6%), and a half-life of 211,000 years (Tagami, 2003, Meena and Arai, 2017). The quantity of $^{99}$Tc produced by nuclear weapons testing in the atmosphere is estimated to be 140 TBq, much of which has

subsequently been deposited and incorporated into sediments (Desmet and Myttenaere, 1986). The concentration of $^{99}$Tc in waste generated after the reprocessing of spent nuclear fuel, which continues to accumulate at active nuclear power stations, is around one kg per ton of U for a conventional boiling water reactor (Artinger et al., 2003, Bruno and Ewing, 2006). The estimated release of $^{99}$Tc by the nuclear power industry through 1986 was on the order of 1000 Bq, mainly the result of releases during nuclear fuel reprocessing. This amount is relatively small compared to the stockpile of $^{99}$Tc associated with spent nuclear materials housed at all of the nuclear power reactors in the United States awaiting final disposition. Significant amounts of $^{99}$Tc were also produced in nuclear reactors that were operated for the production of nuclear weapon materials, mainly Pu and $^{3}$H. For example, at The Department of Energy's Hanford Site in Washington state, nearly 1,990 kg of $^{99}$Tc (1.25 PBq) was produced between 1943 and 1987 (Darab and Smith, 1996). In another example, the inventory of $^{99}$Tc associated with High Level Waste storage at the SRS has been estimated to be 7,600 Curies (Kaplan et al., 1998).

When $^{99}$Tc is released into the environment, plant and animal uptake and the potential for biomagnification in the food chain is a concern (Van Loon et al., 1986). The biological half-life for $^{99}$Tc when consumed, which is the amount of time it takes for half of the $^{99}$Tc to pass through the human body, is roughly 60 hours (Beasley and Lorz, 1986). Because of its low-energy beta-decay, $^{99}$Tc generally poses a limited radiological threat if not ingested. According to the U.S. EPA, the main exposure pathways to humans are by drinking contaminated water and ingestion of contaminated plants. The EPA has set a drinking water standards for $^{99}$Tc at 900 pCi L$^{-1}$. Once $^{99}$Tc enters the body, it will concentrate in the thyroid gland and in the gastrointestinal tract. Even though the body constantly excretes $^{99}$Tc from

the gastrointestinal tract, there is still an increased risk of cancer associated with ingestion (EPA, 2002).

Technetium is a redox-sensitive element that can be found in oxidation states from +2 to +7, of which Tc(IV) and Tc(VII) are the most common in the natural environment (Warwick et al., 2007, Meena and Arai, 2017). The solubility and mobility of Tc in soils is largely determined by its oxidation state, the concentration of organic matter present, and by both biotic and abiotic processes that impact redox conditions (Schulte and Scoppa, 1987). Under aerobic conditions in well-drained surface soils, the oxidized highly water-soluble pertechnetate ($TcO_4^-$) anion will be the predominant species (Coughtrey et al., 1983). Figure 1.3 shows a *Pourbaix* diagram illustrating the dominant aqueous species of Tc as a function of pH and Eh (redox potential) with respect to the thermodynamic stability of water. Technetium (VII) persists under oxidizing conditions, while Tc(IV) is found under reducing/anaerobic conditions as the insoluble Tc-oxy-hydroxide, $TcO_2 \cdot nH_2O_{(s)}$ (Figure 1.4), which persists under neutral to moderately alkaline reducing conditions (Cantrell and Williams, 2012, Cantrell and Williams, 2013). The thermodynamic data for pertechnetate ($TcO_4^-$) is well established; however, our understanding of the Tc aqueous and solids phase speciation in its various valence states is limited.

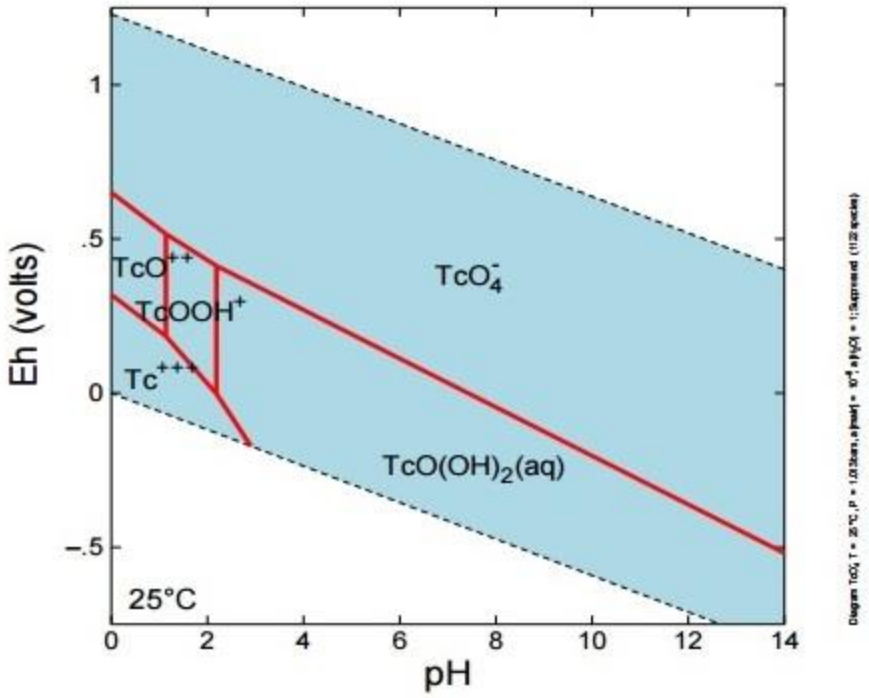


*Figure 1.3: Technetium Pourbaix Diagram. Calculated with Geochemist Workbench using, LLNL thermochemical database with precipitation of solids suppressed. Total [Tc]= 1 x $10^{-8}$ M.*

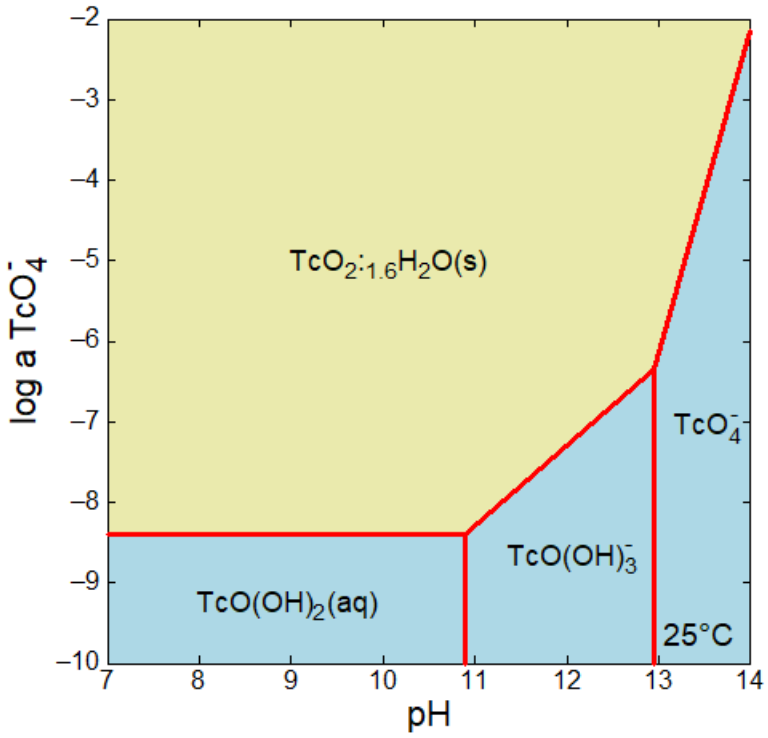


*Figure 1.4: Solubility of $TcO_2 \cdot 1.6H_2O$ as a function of pH at Eh=-0.4V. Calculated with Geochemist Workbench using, LLNL thermochemical database (all other Tc minerals are suppressed).*

Pertechnetate [i.e., Tc(VII)] sorption under aerobic conditions is generally quite limited. Previous laboratory studies on $TcO_4^-$ sorption on subsurface sediments collected from the Savannah River Site (SRS) in Aiken, SC reported $K_d$ values were generally quite low, ranging from -0.13 to 0.29 mL $g^{-1}$, illustrating the limited capacity of such materials to retain $TcO_4^-$ (Kaplan et al., 2000). Further, Tc(VII) $K_d$ values increased with decreasing pH, which was attributed to greater sorption of the Tc(VII) anion by amphoteric Fe and Al oxides. An earlier study by Kaplan et al. (1998) suggested that the negative $K_d$ values measured for Tc(VII) were due to anion exclusion effects for soils with appreciable cation exchange

capacity (Kaplan et al., 1998). Soils from the SRS, however, are generally highly weathered and coarse in texture, with the clay fraction dominated by kaolinite and various amphoteric Fe and Al oxides that can retain anionic solutes (Hu et al., 2005). Another study investigated $K_d$ values for Tc(VII) under oxic conditions for 20 sediment samples from the Hanford Site in Washington. It found $K_d$ values ranged from -0.04 to 0.01 mL $g^{-1}$, indicating no significant sorption under oxic conditions in less weathered subsurface materials (Kutynakov and Parker, 1998).

In sorption experiments using Fe(II)-bearing minerals, Tc(VII) has been observed to reductively precipitate as Tc(IV) (McBeth et al., 2011). When the Tc(IV) was associated with these Fe(II)-bearing minerals, it appears to be somewhat recalcitrant to reoxidation as conditions change. Abdelouas et al. (2005) concluded that in organic matter-rich soils Tc(VII) was reduced and probably precipitated as $TcO_2$, which resulted from a drop in Eh induced by indigenous metal- and sulphate-reducing bacteria. The study also found that organic matter and iron oxyhydroxides play a crucial role in Tc immobilization in soils and that Tc(IV) is strongly complexed with organic matter and bacteria (Abdelouas et al., 2005), illustrating Tc partitioning in soils is strongly influenced by organic matter and the microorganisms that are present.

### 1.4 Rhenium

To avoid the potential danger associate with the radioactive $^{99}Tc$ at high concentrations ($10^{-8}$ to $10^{-4}$ mol $L^{-1}$), researchers have often used Rhenium (Re) as a chemical analogue because of its similar chemical and thermodynamic properties (Kim, 2003, Liu et al., 2013, Lenell and Arai, 2017). Both elements are found in the same row of the periodic table and

possess seven electrons that occupy the outer d and s orbitals, making it possible for these elements to have valence states ranging from 0 to +7. The most stable oxidation state is +7, with the soluble perrhenate ($ReO_4^-$) species that is comparable to pertechnetate ($^{99}TcO_4^-$). Consistent with Tc, the next most stable oxidation state for Re is +4 (Darab and Smith, 1996).

In batch studies comparing the behavior of $^{99}Tc$ and Re under reducing conditions, perrhenate has been observed to be more resistant to chemical reduction by Sn(II) than pertechnetate (Maset et al., 2006). Also, Tc(VII) reduction proceeded during nitrate ($NO_3^-$) reduction in soil microcosm experiments while no Re(VII) reduction occurred, with the applied perrhenate remaining in the solution (Wharton et al., 2000). Both Tc(VII) and Re(VII) are subject to reduction by sulfide ($S^{2-}$); however, perrhenate is still more resistant to reduction than pertechnetate. Thus under reducing conditions, it appears Re(VII) is more difficult to reduce than Tc(VII), and more readily subject to oxidation, making it amore conservative chemical analogue for predicting Tc(VII) behavior in response to transient redox conditions.

### 1.5 Zero Valent Iron

A great deal of research has focused on the removal and/or degradation of groundwater contaminants by using zero-valent iron (ZVI) as a reactive sorbent due to its non-toxicity, abundance, economic feasibility, ease of production, and low maintenance. For example, ZVI has been shown to effectively remove various redox sensitive contaminants from groundwater systems (e.g., Cr, Pb, U, and Mo) (Cantrell et al., 1995, Ponder et al., 2000, Xin et al., 2015).

Several limitations to using ZVI for *in-situ* groundwater remediation as a permeable reactive barrier (PRB) or as a water treatment filter have been observed in previous studies. These limitations include: (1) low reactivity due to its intrinsic passive layer, (2) narrow working pH range, (3) reactivity loss with time due to the precipitation of metal hydroxides and carbonates, (4) low selectivity for the target contaminant, (5) limited efficacy for the treatment of some refractory contaminants and passivity of ZVI arising from certain contaminants, and (6) the potential for sorbed contaminants to be mobilized as the ZVI material ages (Guan et al., 2015, Calderon and Fullana, 2015). Due to these limitations, major concerns remain in the broad application of ZVI based water treatment technologies.

Equation 1.8 shows the initial oxidation of ZVI, resulting in the liberation of two electrons that can react with target contaminants to alter their chemical speciation.

$$Fe^0 \leftrightarrow Fe^{2+} + 2e^- \qquad \text{Eq. 1.8}$$

A common pollutant found in groundwater is nitrate ($NO_3^-$) due to chemical fertilizers, pesticides, animal-feeding operations, petroleum products, and waste contamination through storm and urban runoff (Follett and Hatfield, 2001). Recently, ZVI has been studied for its ability to reduce $NO_3^-$ in water and groundwater. Nitrate can be reduced to $NH_3$ and $N_2$, with Fe oxidized to $Fe^{2+}$ to $Fe^{3+}$ and the subsequent formation of $Fe_2O_3$, $Fe_3O_4$ depending on the reaction conditions (Fu et al., 2014). Under slightly alkaline to acidic conditions, the reduction of $NO_3^-$ to $NH_3$ is spontaneous and rapid, even in an aerobic system at room temperature (Cheng et al., 1997). However, $NO_3^-$ reduction by ZVI is generally limited to acidic conditions or systems in which the solution is buffered to prevent the subsequent

increase in pH. In unbuffered solutions, the pH can increase to >8.0 rapidly, resulting in surface passivation, i.e., surface corrosion, and a dramatic decrease in the rate of $NO_3^-$ reduction (Xu et al., 2012). The reduction of $NO_3^-$ will continue in the presence of mixed valent Fe corrosion products, however, the increasing pH may facilitate the gaseous release of $NH_3$ from alkaline solutions to complete the remediation process.

Recently, Liu et al. (Liu et al., 2013, Lenell and Arai, 2017) and Lenell and Aria (2017) investigated Tc reduction and sorption on ZVI as a possible remediation technique for contaminated groundwater. Using Re as a non-radioactive analogue for Tc, batch and column experiments demonstrated the effective reduction of $ReO_4^-$ by ZVI in simulated groundwater solutions. However, both experiments showed that the rate of $ReO_4^-$ immobilization/sorption decreased significantly as the pH increased from 8 to 10.

To address the limitations associated with ZVI, a high-surface area porous iron composite (PIC) material consisting of both reduced Fe and Fe oxides was recently developed by North American Höganäs for use as both a reactive filtration material for water treatment applications and possibly as an in situ PRB (Hu, 2016). For water treatment, contaminated groundwater is passed vertically up through a column containing the PIC material in order to effectively change the speciation and/or immobilize the target contaminants. The reactive mechanisms responsible for contaminant treatment are quite similar to conventional ZVI; however, the PIC materials have a larger reactive surface area, and are more reactive and efficient at removing target contaminants than traditional ZVI materials. Using the PIC materials, Allred (2012) demonstrated the ability of the materials to reduce a significant amount of $NO_3^-$, sorb orthophosphate ($PO_4^{3-}$), and chemically degrade the herbicide atrazine in agricultural drainage waters (Allred, 2012). More recently, Seaman et al. (2018)

demonstrated the ability of PIC materials to effectively address a range of redox sensitive contaminants as a municipal water treatment strategy (Seaman et al., 2018).

### 1.6 Objectives

The objective of this study was to assess the ability of four commercially available Fe materials (i.e., a novel porous iron composite material, reagent grade Zero Valent Iron, and two commercial Fe oxides) to immobilize Re from contaminated groundwater in the presence and absence of other common oxidants, such as nitrate ($NO_3^-$) and dissolved $O_2$, that are likely present in Tc contaminated systems. This objective was achieved using both laboratory batch and dynamic column experiments.

# CHAPTER 2

# IMMOBILIZATION OF RHENIUM AS A TECHNETIUM ANALOGUE WITH IRON MATERIALS IN BATCH EXPERIMENTS

## 2.1 Introduction

Technetium-99 ($^{99}$Tc), one of several radioactive isotopes of technetium (Tc), is a beta emitter ($\beta^- \approx 249$ keV) with a half-life of 211,000 years that decays to form stable ruthenium-99 ($^{99}$Ru). Technetium-99 is a fission product of uranium-235 ($^{235}$U) in the nuclear fuel cycle, with a fission yield from enriched uranium (i.e., fuel rods of uranium dioxide that contain ~3% $^{235}$U) of 6.03 % (Luykx, 1986, Hu et al., 2010). When fuel rods are no longer usable in the reactor, they are removed from the reactor core and are considered spent nuclear fuel (SNF). These highly radioactive fuel rods continue to generate a great deal of heat and are placed in pools of water to allow them to cool while short lived isotopes decay. Technetium in SNF is immobilized in metallic phases that form in void spaces within fuel rods (Kleykamp, 1985). Buck et al. (2004) performed detailed analysis of SNF and found that very little Tc is sequestered in the $UO_2$ lattice. Therefore, a great deal of $UO_2$ would have to be dissolved to expose the metallic phases to aqueous solution in order to mobilize Tc (Buck et al., 2004). Processing SNF to recover $^{235}$U, $^{239}$Pu, and other fissile elements is the primary way Tc becomes a mobile part of the waste stream. Technetium has found its way into the environment over the last 40 years principally through the approved or accidental discharge

of nuclear fuel processing fluids and other related nuclear materials processing wastes (Schulte and Scoppa, 1987, Hu et al., 2010).

On the Department of Energy's (DOE) Savannah River Site (SRS, Aiken, SC), the processing of nuclear materials used in the production of plutonium (Pu) and tritium ($^{3}H$) has generated a large inventory of radiological waste materials that threaten soil and groundwater resources. Although much of the initial radioactivity is associated with cesium-137 ($^{137}Cs$) and other short lived radioactive components, the long-term future risk drivers at the SRS and other DOE facilities are iodine-129 ($^{129}I$, $t_{1/2}$= 15.7 million years) and $^{99}Tc$ because of their long half-lives and mobility in the subsurface environment (Hu et al., 2010, Icenhower, 2010).

Under oxic conditions, Tc is found in the +7 oxidation state [Tc(VII)] as the oxyanion pertechnetate ($TcO_4$), which is soluble in water and extremely mobile. Under chemically reducing conditions, Tc(VII) may be reduced to lower oxidation states, mainly to Tc(IV), which can precipitate as oxide/oxy-hydroxide and sulfides, i.e., $TcO_{2(s)}$ and $TcO_2 \cdot nH_2O_{(s)}$, and Tc-sulfides depending upon pH and the presence and absence of complexing agents (Lieser, 1993). Due to the radioactivity associated with Tc researchers have often used rhenium (Re) and the perrhenate ($ReO_4^-$) anion as a chemical analogue because both elements share similar physical and chemical properties (Cf Chapter 1, pg 17).

Contaminant extraction and/or groundwater remediation technologies generally focus on changing the chemical speciation of the target contaminant in a manner that reduces mobility and/or bioavailability. Examples include, chemical precipitation, solvent extraction, ion exchange, membrane filtration, adsorption, and chemical reduction (Liang et al., 1996). Because Tc is a redox-sensitive element and its solubility and mobility in subsurface pore

waters depends strongly on its oxidation state, *in situ* reduction of Tc(VII) to Tc(IV) has been proposed as a remediation technology to isolate and/or immobilize Tc in the environment (Istok et al., 2004).

Over the last two decades Zero Valent Iron (ZVI) materials have received considerable attention as versatile reactive sorbents to remediate a range of groundwater contaminants (Fu et al., 2014, Guan et al., 2015, Noubactep, 2014). ZVI has been shown to successfully remediate nitrate (Hwang et al., 2011, Ryu et al., 2011, Jiang et al., 2011), chromium (Qiu et al., 2012, Lv et al., 2012), lead (Zhang et al., 2011), and uranium (Gu et al., 1998) from groundwater. Due to the standard redox potential ($E° = -0.44V$), ZVI it is an effective reductant when reacting with oxidized contaminants such as Cr(VI) and U(VI) (Mitra et al., 2011, Gu et al., 1998, Farrell et al., 1999). The reductive contaminant immobilization mechanism for ZVI involves the transfer of electrons to the contaminant of interest such that it forms a less mobile/toxic species. Other mechanisms for contaminant removal by ZVI include sorption, surface precipitation, and co-precipitation with various iron corrosion products such as ferrous/ferric (hydr)oxides (Mak et al., 2009), which is the case for As(V) removal from groundwater by ZVI (Liu et al., 2009). Since Tc is a redox sensitive species, ZVI has been proposed as a possible reactive material for removing Tc from contaminated groundwater and potentially other waste streams (Lenell and Arai, 2017).

However, several limitations have been observed with the application of ZVI for groundwater treatment. These limitations include: 1) the development of an oxidized passivation layer (e.g., metal hydroxides and metal carbonates) at the materials surface that hinders continued effectiveness and reduces hydraulic conductivity; 2) the narrow effective pH range for select target contaminants; 3) the low selectivity for certain contaminants of

interest under oxic conditions in the presence of alternate electron acceptors; and 4) the limited effectiveness for certain contaminants (Fu et al., 2014, Guan et al., 2015, Noubactep, 2014).

The objective of this study was to assess the ability of four commercially available Fe materials (i.e., a novel porous iron composite material, reagent grade Zero-Valent Iron (ZVI), and two commercial Fe oxides) to immobilize Re from contaminated water in the presence and absence of common oxidants, such as nitrate ($NO_3^-$) and dissolved $O_2$ that are likely present in Tc contaminated systems.

## 2.2 Materials and Methods

Due to the potential hazard and constraints of working with radionuclides, Re is often used as a surrogate for Tc in experiments (Kim and Boulègue, 2003, Brookins, 1986, Ding et al., 2013, Pierce et al., 2014, Poineau et al., 2006). For this experiment Re is used as an analogue for Tc in batch sorption experiments. Two sets of batch experiments were carried out, one using $NaReO_4$ (4 ppm Re) and the other using $NaReO_4$ plus $NaNO_3$ (100 ppm $NO_3^-$) to determine if $NO_3^-$ is an effective competitor for both the chemical reduction capacity of the PIC and ZVI materials, and the anion sorption capacity of those materials plus the two Fe oxide treatments.

### 2.2.1 Stock solutions

Stock solutions of $NaReO_4$ were made by dissolving 0.22 g $NaReO_{4(s)}$ in 1 L of milliQ water resulting in a 150 ppm solution of $Re_{(aq)}$. A NaCl stock solution was made by dissolving 58 g $NaCl_{(s)}$ in 1 L milliQ water, resulting in a 1.0 M NaCl solution. A 1.0 M $NO_3^-$

solution was made by dissolving 42 g $NaNO_{3(s)}$ in a 500-mL volumetric flask brought to volume using milliQ water.

The stock solution of 4 ppm Re (Solution A) was made by mixing 53 mL of 150 ppm $Re_{(aq)}$ with 20 mL 1.0M NaCl in a 2.0-L volumetric flask, the flask was brought to volume using milliQ water. Approximately 8.0 L of solution A was made up.

For the solution of 4 ppm Re and 100 ppm $NO_3^-$ (Solution B), 53 mL of the 150 ppm Re, 2.35 mL of the 1.0M $NaNO_3$, and 17.65 mL of the 1.0 M $NaCl_{(l)}$ were mixed together in a 2.0 L volumetric flask brought to volume with milliQ water.

*Table 2.1: Final Concentrations of Stock Solutions*

| | Treatment Solution A | Treatment Solution B |
|---|---|---|
| Re (mg $L^{-1}$) | 4.0 | 4.0 |
| $NO_3^-$ (mg $L^{-1}$) | | 100 |
| $Na^+$ (mg $L^{-1}$) | 230 | 230 |
| $Cl^-$ (mg $L^{-1}$) | 354 | 312 |

### 2.2.2 Iron

Four Fe-based reactive sorbents were evaluated in the current study. The most novel of the test materials is a high-surface area porous iron composite (PIC) material consisting mainly of $Fe^0$ and Fe oxides, produced by North American Höganäs through a proprietary process (Specific Surface Area = 10 $m^2$ $g^{-1}$) (Hu, 2011). To date this material has been proposed for waste water treatment in a limited set of laboratory tests in applications that are similar to ZVI (Hu, 2011, Seaman et al., 2018). The mechanisms of contaminant immobilization and/or degradation are quite similar to conventional ZVI, except the PIC

material has a much larger reactive surface area, and limited testing has shown it to be more effective than conventional ZVI at removing a range of target contaminants ($NO_3^-$, Re, Sr, Ra, As, and U) (Seaman, 2015, Seaman et al., 2018). The second material is Reagent Grade Zero-Valent Iron (ZVI) supplied by Sigma-Aldrich (Particle Size = >0.15 mm). The third material, Bayoxide® E33 (GFH1), made by Advant Edge Technologies, Inc. from Beauford, GA, is an Fe based granular media primarily used for the removal of As(III) and As(V) from contaminated water (Particle Size = 2.00 x 0.50 mm; Bulk Density = 0.46 – 0.57 g $cm^{-3}$; Surface Area = 120 – 200 $m^2$ $g^{-1}$). It is described by the manufacturer as an akaganeite-like mineral adsorbent, characterized as poorly crystallized β-FeOOH with an intraparticle porosity of ≈ 70-80% (Badruzzaman et al., 2004). The fourth material, GFH® Granular Ferric Hydroxide (GFH 2), is also an Fe-based media manufactured by Evoqua Water Technologies based out of Pittsburg, PA (Particle Size = 2.00 x 4.00 mm; Bulk Density = 0.46 – 0.58 g $cm^{-3}$). This material is primarily used for the removal of As(III), As(V), and other heavy metals from contaminated water (Evoqua, 2014).

### 2.2.3 Re(VII) Reduction/Sorption in the Presence and Absence of $NO_3^-$

An initial set of batch experiments was carried out using the 4 ppm Re solution (Solution A, Table 2.1). A subsequent batch test was carried out using a test solution that contained both 4 ppm Re as $ReO_4^-$ and 100 ppm $NO_3^-$ as a competitive oxidized species (i.e., Solution B, Table 2.1).

The reaction vessels for this experiment were 250-mL disposable plastic beakers. Each treatment was carried out in triplicate, including no sorbent control beakers in both oxic (i.e., lab atmosphere) and anoxic (5% $H_{2(g)}$ and 95% $N_{2(g)}$ atmosphere) environments (Coy Vinyl

Anaerobic Chambers, Grass Lake, MI). For each treatment, 10g of sorbent material (PIC, ZVI, GFH1, and GFH2) were placed in the reaction vessel along with 200mL of the appropriate treatment solution (i.e., with, solution A and without $NO_3^-$, solution B). The experimental controls contained only the 200mL treatment solution and no sorbent material. For the anoxic experiment, the Fe materials were weighed out and equilibrated in the anoxic chamber over night before the experiment began. Anoxic treatment solutions were bubbled inside the anoxic chamber for 30 minutes to remove any dissolved $O_2$. Once the 200mL of treatment solution was added to each reaction vessel they were placed on an orbital shaker and equilibrated at approximately 140 rotations per minute. Both the oxic and anoxic treatment remained open to the equilibrating treatment atmosphere.

Non-destructive samples for chemical analysis (a total of 2.75% of the solution) were taken from each reaction vessel at 1, 3, 6, 12, 24, 48, 120, 164, 360, 480, and 720 hours. During sampling, 0.5 mL of solution was removed from each reaction vessel, and then the pH and ORP of the residual solution in the reaction vessel was measured. The samples were diluted with milliQ water, filtered (0.22µm pore size filter), and acidified (2% $HNO_3$) for chemical analysis of Re and Fe concentrations by inductively coupled plasma mass spectrometry (ICP-MS) on a Nexlon 300 (Perkin Elmer, Inc.) in accordance with the quality assurance (QA) and quality control (QC) protocols of EPA method 6020A (USEPA, 2007b). Non acidified samples were analyzed as follows: $NO_3^-$ was determined by the Chromotropic Acid test method, nitrite ($NO_2^-$) was determined by the Diazotization method (APHA, 1997b), and ammonia/ammonium ($NH_4^+/NH_3$) was determined by the Phenate method (APHA, 1997a).

### 2.2.4 Solid Phases analysis

The raw materials were characterized by X-Ray Diffraction (XRD) analysis using a Bruker D-2 Phaser operating at 30 kV and 10 mA using Cu K-alpha radiation ($\lambda = 1.5406$ A) over an angular range of 10° to 90° 2θ with a step scan size of ≈ 0:014° $sec^{-1}$ using the Bragg-Brentano geometry.

### 2.2.5 Statistics

Statistical tests were conducted using ANOVA to determine whether or not the means of several treatment groups are significantly different, and therefore generalizes the Student t-test to more than two groups. ANOVAs were used here for comparing more than two means. In some cases, we evaluated the probability that the means of two populations were equal using a Tukey post-hoc test to address multiple comparisons. All of the statistical analysis for the current study were performed using R 2.14.0 (R Development Core Team, 2013).

## 2.3 Results

### 2.3.1 Phase characterization

Based on XRD analysis four iron materials were comprised as follows: the ZVI was determined to be composed at 100% of Zero-Valent Iron; the PIC material is composed of 90% Zero-Valent Iron, with ≈ 10% composed of the mixed-valence Fe oxides with a formula of $Fe_3O_4$; GFH1 is composed of goethite (α-FeOOH) and antigorite $(Mg, Fe)_3(Si_2O_5)(OH)_4$) and the GFH2 is composed of Iron Hydroxide (FeOOH).

### 2.3.2 Rhenium immobilization in oxic and anoxic environments

#### 2.3.2.1 pH and ORP

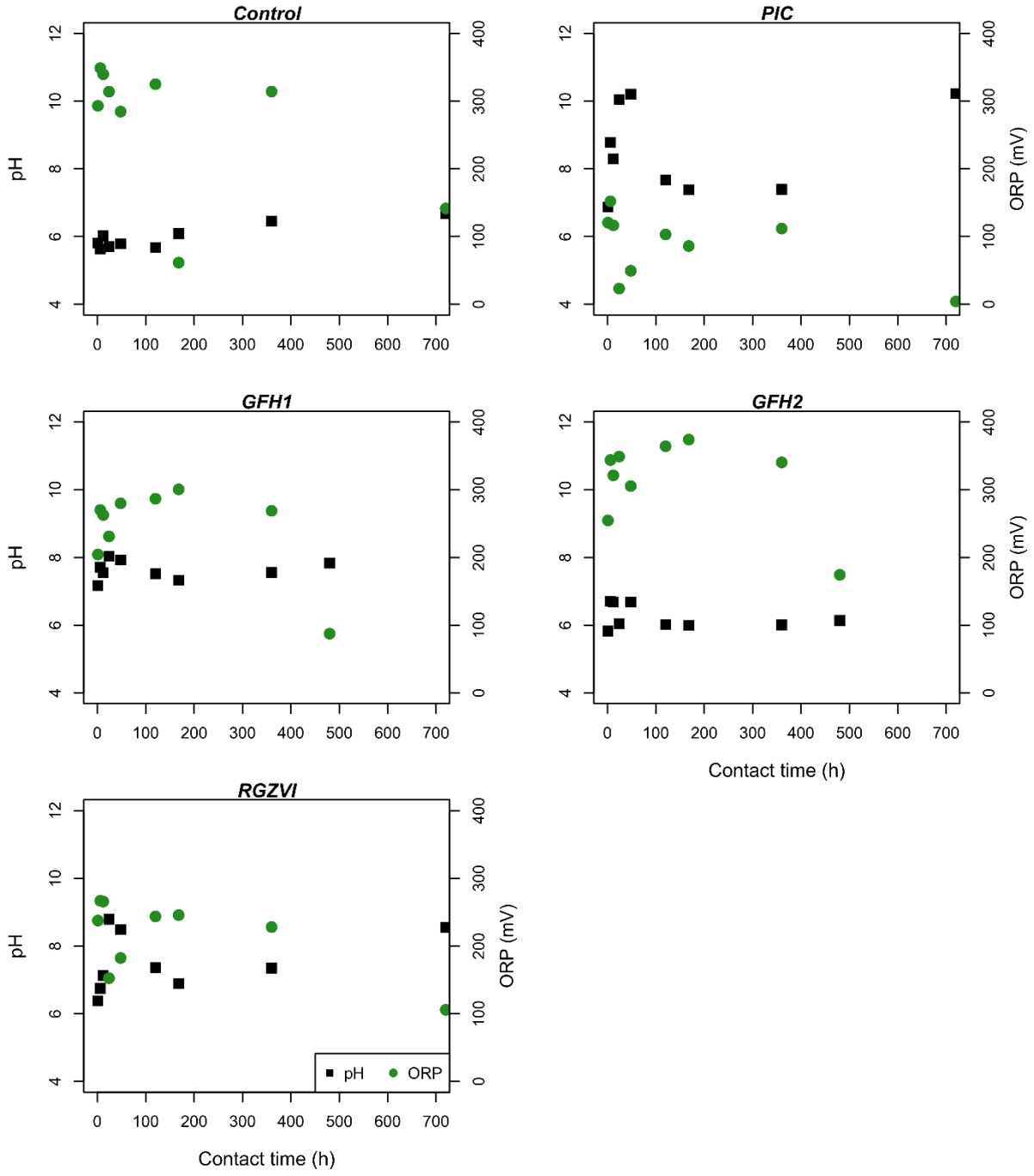


*Figure 2.1: Batch pH and ORP values for treatment solutions without $NO_3^-$ and open to the atmosphere (oxic)*

Figure 2.1 shows the pH and Oxidation Reduction Potential (ORP) of the treatment solutions versus the contact time (in hours) for the control, PIC, ZVI, GFH1, and GFH2 treatments in the oxic environment. In general, the addition of the Fe-based sorbent materials significantly increases the pH of the solution compared to the control with the exception of GFH2. Under oxic conditions the pH of the control remains between ≈ 5.6 and 6.7, appearing to increase somewhat over time. For the PIC treatment, the pH begins increasing above the no sorbent control within the first hour and continues to increase throughout the equilibration time ending with a pH of ≈ 10.2. For the ZVI treatment, the pH begins to increase within the first hour and continues to increase for the first 24 hours, it then remains between ≈ 6.9 and 8.6, ending with a pH of ≈ 8.5. For the GFH1 treatment, the pH goes above the control within the first hour and remains between ≈ 7.2 and 8.0, ending on ≈ 7.8. For the GFH2 treatment, the pH is initially similar to that of the control until hour 3 and then increases to ≈ 6.7, where it remains throughout the experiment.

For the control under oxic conditions, the ORP was initially ≈ 293 mV and increases to ≈ 349 mV at hour 6, and then fluctuates between ≈ 61.4 mV and 340 mV, ending on ≈ 141 mV. For the PIC treatment, the ORP starts below the control and continues to decrease over time, ending at ≈ 4.1 mV. For the ZVI treatment, the ORP is generally lower than the control. However, it does increase to ≈ 266 mV then decreases to ≈ 106 mV by the end of the experiment. For the GFH1 treatment, the ORP is below the control, but it increases until hour 164 to ≈ 301 mV, and then decreases to ≈ 87.3 mV at the end of the experiment. For the GFH2 treatment, the ORP is initially lower than that of the control until hour 24 when it goes above the control until hour 164 with a value of ≈ 374 mV it stays above the control and ends with ≈ 174 mV. For the ORP, there is considerable variation at the beginning of the

experiment. Clearly the ZVI and PIC materials decrease the ORP more compared to the control and the GHF1 and GFH2 materials.

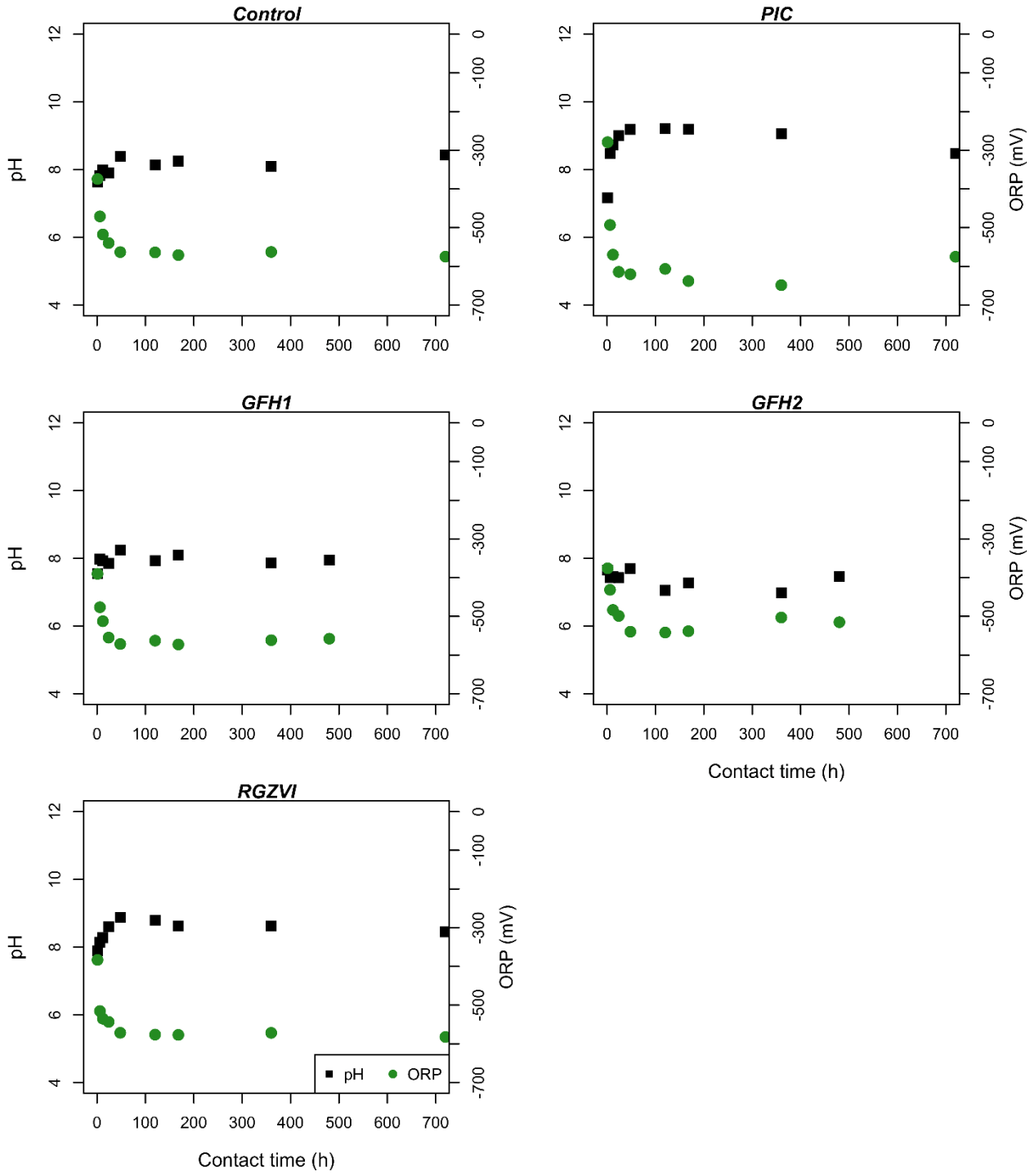


*Figure 2.2: Batch pH and ORP values for treatment solutions without $NO_3^-$ in the anoxic environment*

Figure 2.2 shows the pH and ORP of the solution treatments versus the contact time (in hours) for the no sorbent control, PIC, ZVI, GFH1, and GFH2 treatments in the anoxic environment. For the anoxic test conditions, there was an initial decrease in ORP for all sorbent treatments and the no sorbent control. For the PIC and ZVI sorbents, the decrease in ORP is also associated with an increase in pH. For the two Fe oxide sorbents and the control, the pH remains fairly constant throughout equilibration. Under anoxic conditions the pH of the control ranges between ≈ 7.2 and 8.4. For the PIC treatment, the initial pH is below the control, but then increases to ≈ 9.2 at hour 120, with a final pH of ≈ 9.1 at the end of the experiment. The ZVI treatment pH stays the same as the control pH until the 24-hour sampling point when the pH increases above the control to ≈ 8.6 to 8.9, with a final pH at the end of the experiment of ≈ 8.6. The GFH1 treatment pH essentially stays the same as the control pH throughout the experiment. The GFH2 treatment pH is also quite similar to the control until hour 164 when it decreases to 7.3, eventually ending at a pH of ≈ 7.06. For each of the treatments, the pH increases and continues to until the 164-hour sample point when the pH decreases, with the exception of GFH1 and GFH2 which the pH remains the same as the control pH.

As expected, the ORP values for the treatment solutions in the anoxic environment were consistently lower than the values observed for the oxic environment, regardless of the sorbent treatment, with final ORP values that are quite similar for all treatments. For the control, the ORP is initially ≈ -374 mV and decreases to ≈ -564 mV at the 120-hour sampling point, with a final ≈ - 562 mV ORP reading at the end of the experiment. For the PIC treatment, the ORP is initially above the control at ≈ -279 mV, but then decreases below the control at the 12-hour sampling point with an ORP of ≈ -570 mV. The ZVI treatment ORP

stays the same as the control until the 48-hour sampling point when it decreases below the control with an ORP of ≈ -572 mV and continues to decrease until the end of the experiment. The GFH1 treatment ORP is the same as the control until the 48-hour sampling point when it reaches ≈ -572 mV. The ORP continues to decrease below the control ending with an OPR of ≈ -573 mV. The GFH2 treatment ORP is quite similar to that of the control throughout the experiment.

#### 2.3.2.2 Re sorption

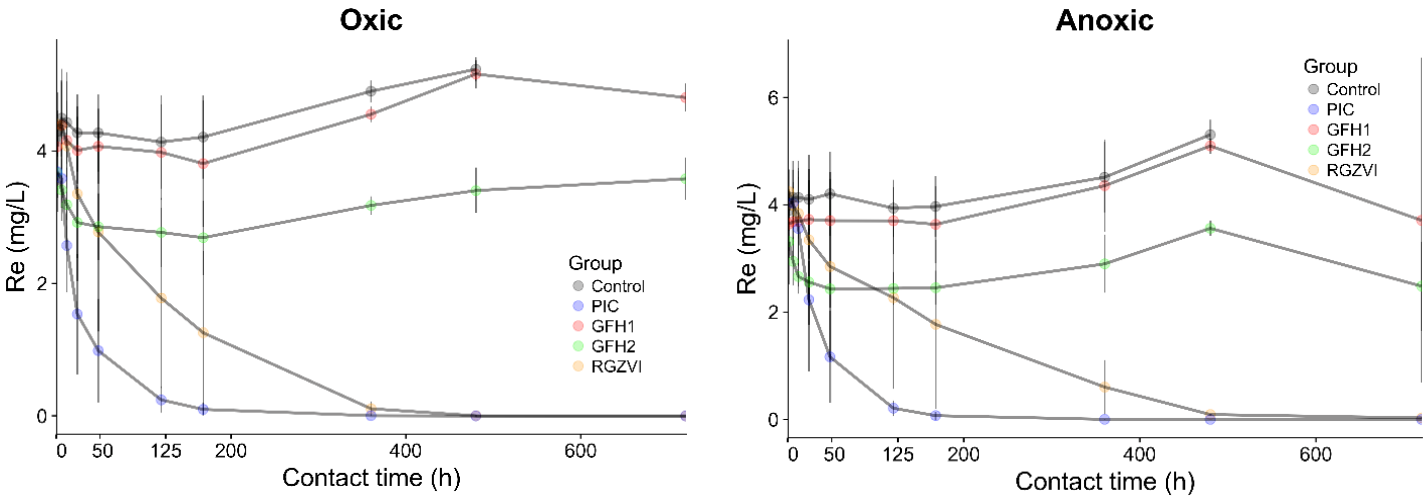


(a) (b)

*Figure 2.3: Rhenium in solutions without $NO_3^-$ in the oxic (a) and anoxic (b) test conditions, shown with a 95% confidence intervals.*

Figure 2.3 shows the Re concentration (in mg $L^{-1}$) versus the contact time (in hours) for the control, PIC, ZVI, GFH1, and GFH2 and treatments in oxic (a) and anoxic (b) environments for solutions without $NO_3^-$. The Re results are remarkably similar under both treatment atmospheres. Under oxic conditions, the initial Re concentration was for the control was 3.99 ± 0.05 mg $L^{-1}$ and remains constant or even apparently increases over time, i.e., $t_{480h}$ Re = 4.81 ± 0.17 mg $L^{-1}$. This apparent increase in Re observed for the control and GFH1 treatments is likely due analytical error. The PIC treatment is apparently faster at removing Re from solution than the other sorbent, including the ZVI, regardless of the treatment atmosphere. The ZVI treatment is the second most effective of the tested sorbent at removing Re from solution. For the PIC treatment, the Re concentration is the same as the control for the first sampling time, but by hour 6 the concentration started to decrease below the control. The concentration decreases to 2.14 ± 0.88 mg $L^{-1}$ at the 12-hour sampling point, from there the concentration decreases until it was no longer detectable in solution by hour 480. For the ZVI treatment, the Re concentration was statistically the same as the control for the first hour sampling, by hour 6 the concentration was 3.36 ± 0.09 mg $L^{-1}$ which below the control, and continues to decrease to 3.10 ± 0.24 mg $L^{-1}$ at the 12-hour sampling, the concentration continues to decrease until it is no longer detectable at the end of the experiment. For the GFH1 treatment (Bayoxide), the residual Re concentration was statistically the same as the control throughout the duration of the experiment. The Re concentration for hour 360 and 480 show 4.52 ± 0.41 mg $L^{-1}$ and 5.10 ± 0.21 mg $L^{-1}$, respectively, since this concentration is greater than the initial Re concentration for the solution, and likely the result of analytical error. For the GFH2 treatment, the Re concentration remaining in solution decreases below that of the control statistically within the

first hour. It and continues to decrease to 2.70 ± 0.10 mg $L^{-1}$ at the 12-hour sampling point, the concentration is 2.22 mg $L^{-1}$ at the 168-hour sampling point. The last two sample times, 360 hours and 480 hours, the concentration was 3.09 ± 0.31 mg $L^{-1}$ and 3.40 ± 0.34 mg $L^{-1}$, respectively, which could be associated with Re desorption or analytical error.

Under anoxic conditions, the no sorbent control was initially 4.01 ± 0.17 mg $L^{-1}$ and remained stable. For the PIC treatment, the Re concentration was the same as the control for the first hour, afterwards the concentration decreases below the control, and decreases significantly for the next 23 hours to reach 1.07 ± 0.26 mg $L^{-1}$ and continues to decrease until the concentration is no longer detectable by hour 168. On the ZVI treatment, the Re concentration is the same as the control for the first hour sample time. The concentration then decreases below the control concentration reaching 3.63 ± 0.02 mg $L^{-1}$ at hour 6, the concentration continued to decreases until the end of the equilibration time at 720 hours with a concentration of 0.02 ± 0.01 mg $L^{-1}$. For the GFH1 treatment, the Re concentration stays the same as the control until the 24-hour sampling point when the concentration decreases reaching 3.53 ± 0.01 mg $L^{-1}$. The concentration decreases until the 360-hour sampling point when the concentration exceeds the initial concentration, due to analytical error, at 4.78 ± 0.56 mg $L^{-1}$ and again the concentration increases to 5.09 ± 0.14 mg $L^{-1}$ at the 480-hour sampling point. For the GFH2 treatment, the Re concentration is below the control concentration at 3.62 ± 0.05 mg $L^{-1}$, the concentration continues to de crease to 3.12 ± 0.13 mg $L^{-1}$ at hour 6 sampling point and remains stable until the 360-hour sampling time when the concentration reaches 3.28 ± 0.37 mg $L^{-1}$ and remains stable until the end of the experiment.

#### 2.3.2.3 Statistical analysis

An analysis of variance (ANOVA) using a linear model was run to compare the mean concentration of Re of all the groups to the no sorbent control. The results (Table 2.2) show that the predicted concentration of Re in the no sorbent control is 4.13 ± 0.13 mg $L^{-1}$, which is the baseline. The GFH1 group is 0.18 ± 0.18 mg $L^{-1}$ lower than the baseline, which is not a significant difference; Pr(>|t|) 0.334 > 0.05. For the PIC group the mean Re concentration is 2.94 ± 0.18 mg $L^{-1}$ below the baseline, which is a significant difference; Pr(>|t|) 2e-16<0.05. For the GFH2 group, the Re concentration is 1.25 ± 0.19 mg $L^{-1}$ below the baseline, which is not a significant difference; Pr(>|t|) 9.76e-11<0.05. For the ZVI group the baseline is 2.57 ± 0.18 mg $L^{-1}$ below the baseline, which is significant; Pr(t>|t|) 2e-16<0.05. For the effect of environment, there is no significant difference in Re concentration; Pr(>|t|) 0.545<0.05 (Figure 2.4). The Re concentration in the PIC and ZVI treatments are significantly lower than Re concentration in the control, which signifies that Re is being sorbed to the iron material. The Re concentration in GFH1 and GFH2 is not significantly different than that of the control, which means there is no sorption occurring in these two treatments.

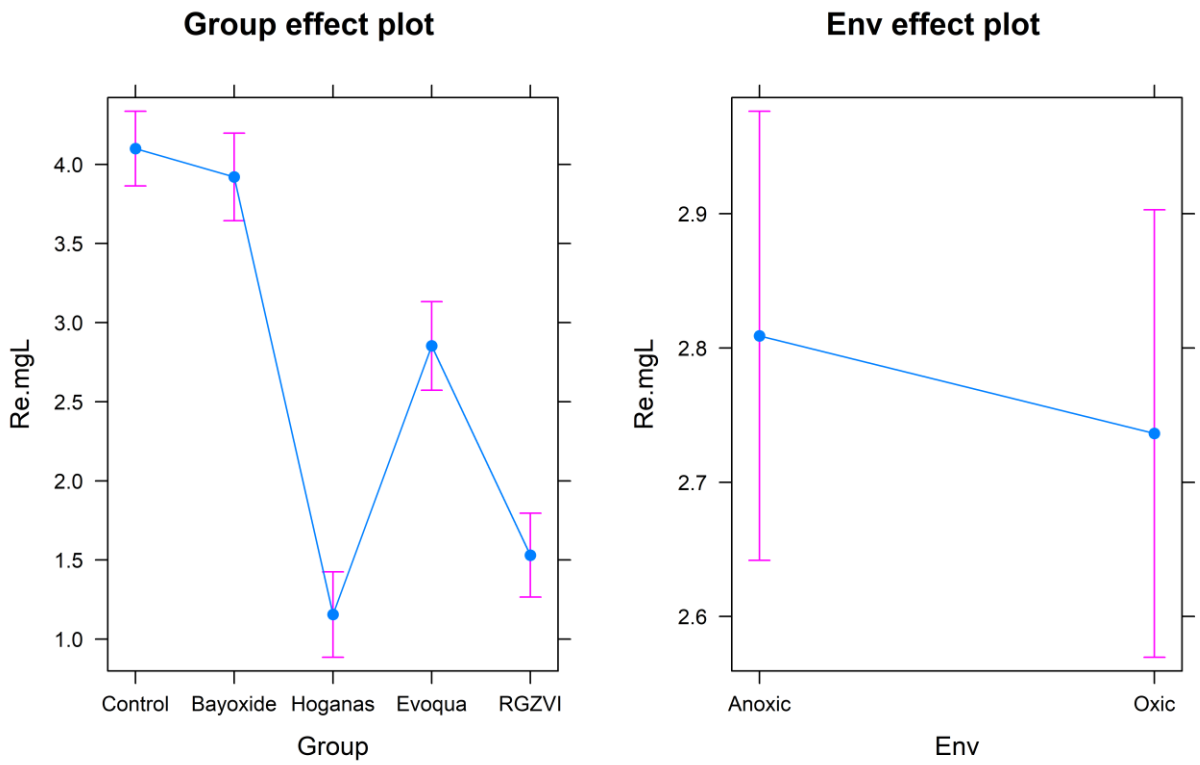


*Figure 2.4: Results of an ANOVA test comparing the mean Re concentrations of all groups to the Re concentration in the control for experiments without $NO_3$*

*Table 2.2: Computer output of ANOVA test comparing the mean Re concentrations of all groups to the Re concentration in the control for experiments without $NO_3$*

| | Estimated | Standard Error | t Value | Pr (>\t\) |
|---|---|---|---|---|
| **(Intercept)** | 4.14 | 0.13 | 30.882 | <2e-16 |
| **GFH1** | -0.18 | 0.18 | -0.968 | 0.334 |
| **PIC** | -2.94 | 0.18 | -16.176 | <2e-16 |
| **GFH2** | -1.25 | 0.19 | -6.712 | 9.76e-11 |
| **ZVI** | -2.57 | 0.18 | -14.250 | <2e-16 |
| **Oxic** | -0.07 | 0.12 | -0.606 | 0.545 |

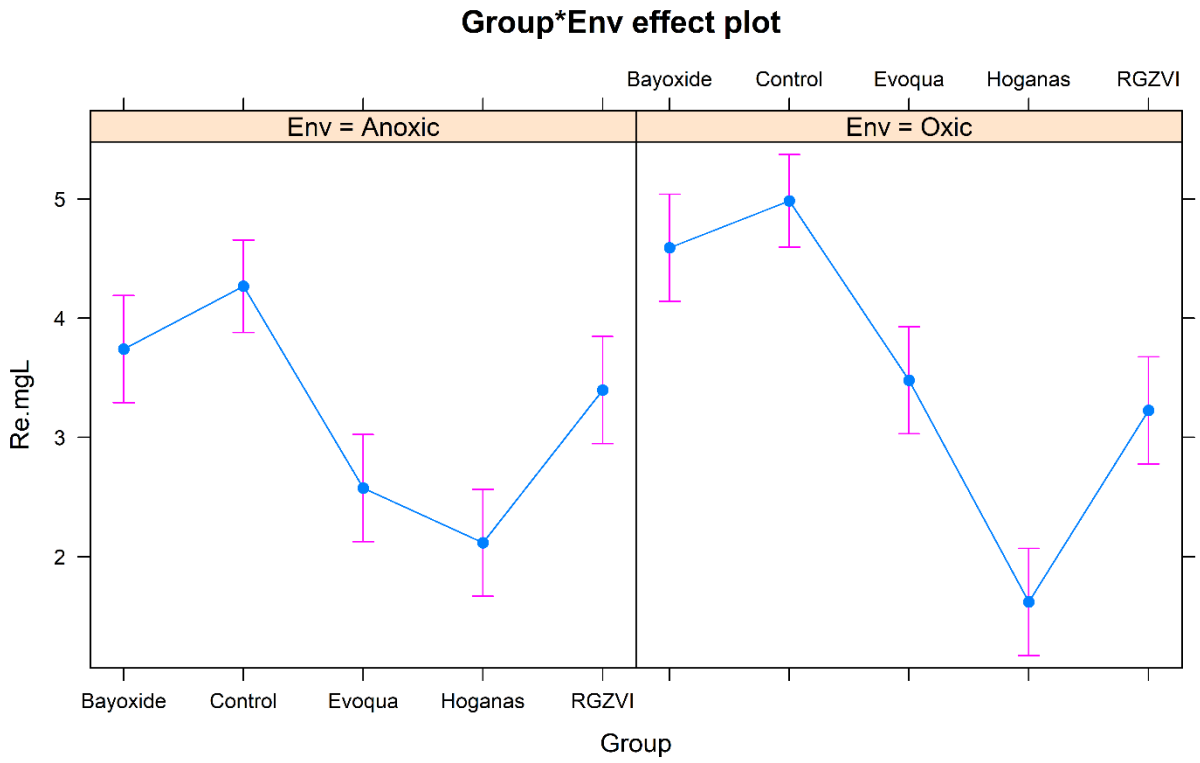


*Figure 2.5: Results of ANOVA linear regression to determine if there was a significant effect on Re concentration in experiments without $NO_3^-$ due to the treatment atmosphere i.e., presence or absence of $O_2$*

Another ANOVA test was run to compare the mean concentration of Re for of all the treatment groups to the control in both the oxic and anoxic environments in the absence of $NO_3^-$. The results are presented in Table 2.3. The predicted Re concentration in the control is 3.74 mg $L^{-1}$, which is the baseline (The intercept is the estimate of the dependent variable (control) when all the independent variables are 0 (Table 2.3)). For the Anoxic environment, the no sorbent control is 0.53 ± 0.30 mg $L^{-1}$ above the baseline, which is not significantly different; Pr(>|t|) 0.08 > 0.05. For GFH2 group the Re concentration is 1.16 ± 0.32 mg $L^{-1}$

below the baseline, which is significantly different; Pr(>|t|) 0.00<0.05. For PIC the Re concentration is 1.62 ± 0.32 mg $L^{-1}$ below the baseline, which is significantly different; Pr(>|t|)<8.45e-07<<<<0.05. For ZVI the Re concentration is 0.34 ± 0.32 mg $L^{-1}$ below the baseline, which is not significantly different; Pr(>|t|) 0.29>0.05. For the comparison of the oxic to anoxic environments, the Re concentration is 0.85 ± 0.32 mg $L^{-1}$ above the baseline, which is not significantly different; Pr(>|t|)0.01<0.05. Under the oxic environments, the mean Re concentration in the control is 0.13 ± 0.43 mg $L^{-1}$ below the baseline, this difference is not significant; Pr(>|t|)0.75>0.05. For GFH2 the Re concentration is 0.05 ± 0.46 mg $L^{-1}$ above the baseline, this difference is not significant; Pr(>|t|)0.91>0.05. For PIC the Re concentration is 1.35 ± 0.46 mg $L^{-1}$ below the baseline, this difference is not significant; Pr(>|t|)0.00<0.05. For ZVI the Re concentration is 1.02 ± 0.46 mg $L^{-1}$ below the baseline, this difference is not significant; Pr(>|t|)0.03<0.05. When comparing each treatment between environments, there is no significant difference, therefore, there is no significant effect of the environment on the Re concentration (Figure 2.5). In the oxic environment, there is a significant difference between the Re concentration between the baseline, PIC, and GFH1 treatment.

Table 2.3: *Computer output of ANOVA test comparing the mean Re concentrations of all groups to the Re concentration in the control for experiments under both oxic and anoxic conditions in the presence of $NO_3$*

| | **Estimate** | **Std. Error** | **t value** | **Pr(>\|t\|)** |
|---|---|---|---|---|
| **(Intercept)** | 3.74 | 0.23 | 16.41 | <2e-16 |
| **Anoxic Control** | 0.53 | 0.30 | 1.75 | 0.08 |
| **Anoxic GFH2** | -1.17 | 0.32 | -3.65 | 0.00 |
| **Anoxic PIC** | -1.62 | 0.32 | -5.04 | 8.45e-07 |
| **Anoxic ZVI** | -0.34 | 0.32 | -1.06 | 0.29 |
| **Oxic** | 0.85 | 0.32 | 2.64 | 0.01 |
| **Oxic Control** | -0.14 | 0.43 | -0.32 | 0.75 |
| **Oxic GFH2** | 0.05 | 0.46 | 0.12 | 0.91 |
| **Oxic PIC** | -1.35 | 0.46 | -2.96 | 0.00 |
| **Oxic ZVI** | -1.02 | 0.46 | -2.24 | 0.02 |

### 2.3.3 Effect of Nitrate on Rhenium immobilization

#### 2.3.3.1 pH and ORP

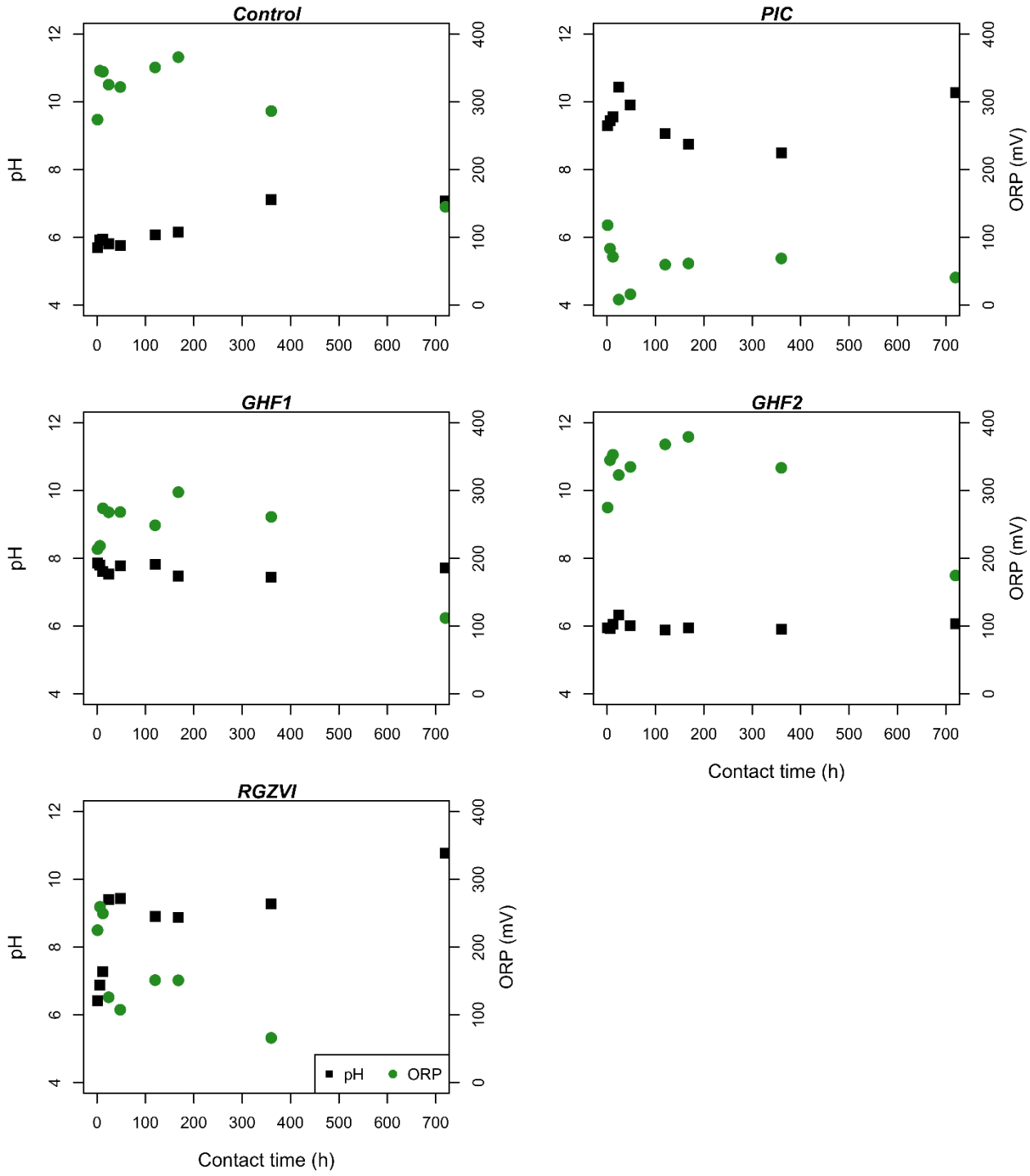


*Figure 2.6: Batch pH and ORP values for the treatment of solutions with $NO_3^-$ in the oxic environment*

Figure 2.6 shows the pH and ORP of solution treatments with $NO_3^-$ versus the contact time (in hours) for the no sorbent control, PIC, ZVI, GFH1, and GFH2 treatments in the oxic environment. The pH for the no sorbent control starts at ≈ 5.7 and oscillates between ≈ 5.8 and 7.1 throughout the experiment. The pH for the PIC treatment is above the control pH throughout the experiment. The pH is ≈ 9.3 at the first hour sampling event then increases to ≈ 10.4 at the 24-hour sampling event. The pH then oscillates between ≈ 8.5 and 10.3 for the remainder of the experiment. The pH for the ZVI treatment stays the same as the control until the 12-hour sampling time, with a pH of ≈ 7.3. The GFH1 treatment pH is above the control pH throughout the experiment, with a pH of ≈ 7.9 at the first hour and increasing to ≈ 8.0 by hour 24. The pH then oscillates between ≈ 7.4 and 7.8 till the end of the experiment. For the GFH2 treatment, the pH is the same as the control pH throughout the experiment. The pH then increases to the end of the experiment with a pH of ≈ 10.8. For the PIC and ZVI, the pH increased overall throughout the experiment.

As observed above for the $NO_3^-$ free treatments, there is more scatter in the ORP values for the oxic treatment atmosphere than in the anoxic. Such scatter may be indicative of the lack of full $O_2$ equilibration throughout the batch reactor, resulting in redox gradients that make consistent, repeated ORP measurements difficult. The no sorbent control ORP oscillates between ≈ 274 mV and 366 mV until hour 120, then decreases to ≈ 145 mV by the end of the experiment. The ORP for PIC stays below the control. It begins to decreases by the first hour sampling event with an ORP of ≈ 121 mV, the ORP continues to decrease to ≈ 8.0 mV at hour 24. The ORP increases to ≈ 68.0 mV at hour 360 then decreases to the end of the experiment to ≈ 40.6 mV. The ZVI treatment ORP stays the same as the control until the 24-hour sampling point with an ORP of ≈ 126 mV. The ORP stays below the control for the

remainder of the experiment ending with an ORP of ≈ 13.1 mV. The ORP for GFH1 is below the control by the first hour sampling with an ORP of ≈ 214 mV, then oscillates between ≈ 112 mV and 298 mV throughout the experiment. The ORP for the GFH2 treatment is the same as the control until the 120-hour sampling event when it goes above the control with an ORP of ≈ 368 mV. The ORP continues to stay above the control for the remainder of the experiment. For the PIC and ZVI, the pH increased overall throughout the experiment as might be expected based on the $Fe^0$ mechanism of reaction with both Re(VII) and $NO_3^-$ (Eq 2.2 and 2.3).

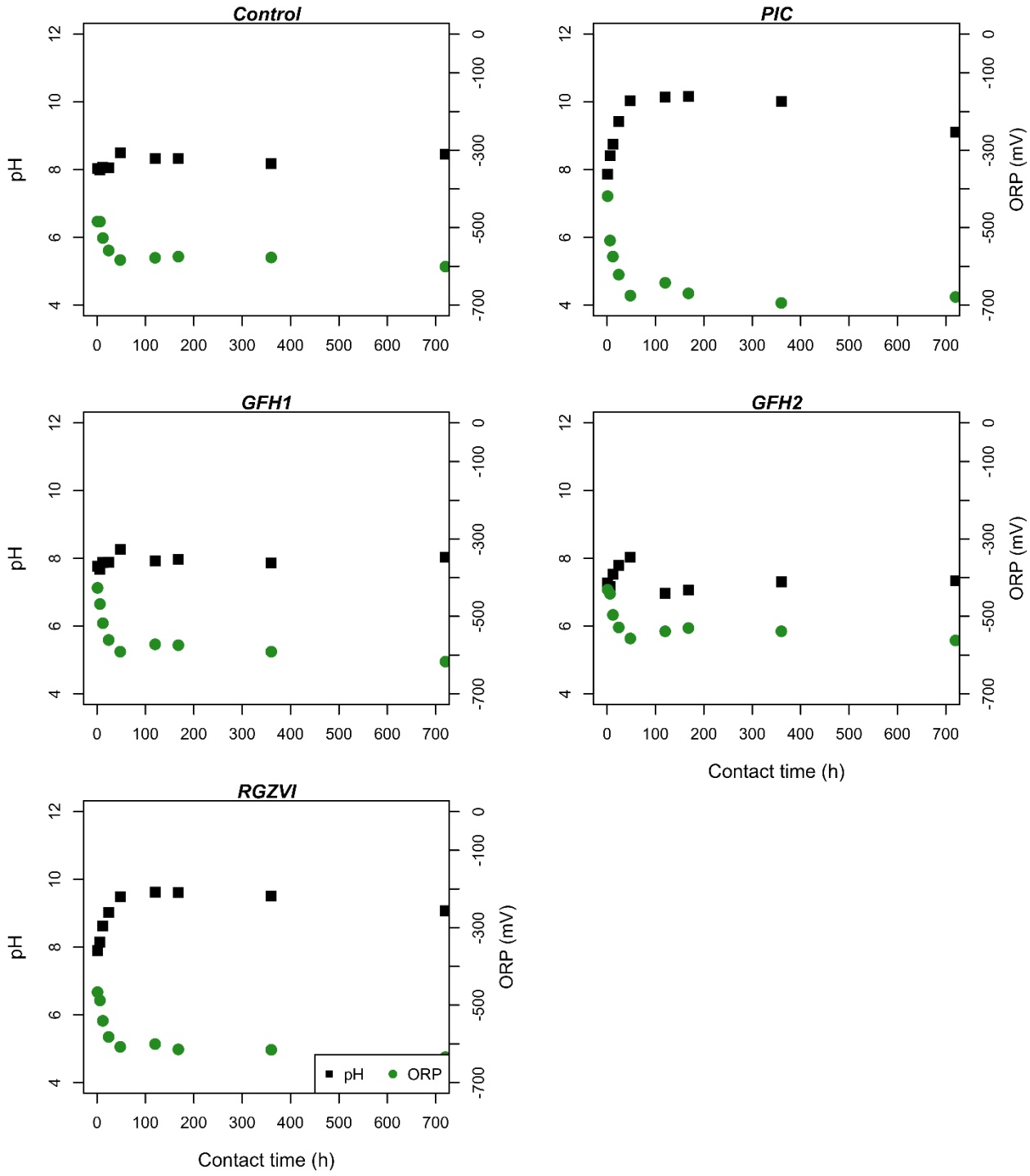


*Figure 2.7: Batch pH and ORP values for treatment solutions with $NO_3^-$ in anoxic environment*

As observed above, there is less scatter in both the pH and ORP values for the anoxic treatment atmosphere. Figure 2.7 shows the pH and ORP of solution treatment $NO_3^-$ versus the contact time (in hours) for the no sorbent control, PIC, ZVI, GFH1, and GFH2 treatments in the anoxic environment. The pH for the no sorbent control remains between ≈ 8.0 and 8.5 throughout the experiment. For the PIC treatment, the first hour sampling point pH is below the control, but increases above the control by hour 12 with a pH of ≈ 8.8. The pH continues to increase reaching ≈10.2 at hour 164, then decreases to ≈ 10.0 at the end of the experiment. The pH for the ZVI is below the control for the first sampling event with a pH of ≈ 7.9, the pH then increases above the control at hour 12 with a pH of ≈ 8.6. The pH remains above the control until the end of the experiment with a final pH of ≈ 9.5. The pH for the GFH1 treatment is below the control at the first hour sampling with a pH of ≈ 7.8. The pH then increases above the control at hour 48 with a pH of ≈ 8.3. The pH then decreases to the same pH as the control and stabilizes to the end of the experiment. The pH of the GFH2 treatment stays below the control pH throughout the experiment.

The ORP of the control starts at ≈ -484 mV and oscillates between ≈ -513 mV and -584 mV throughout the remainder of the experiment. The PIC treatment ORP is above the control ORP for the first hour sampling. The ORP decreases until it is below the control at hour 24 with an ORP of ≈ -622 mV. The ORP continues to decrease to the end of the experiment with an ORP of ≈ -695 mV. For the ZVI treatment, the ORP is below the control until the 6-hour sampling event with an ORP of ≈ -488 mV. The ORP continues to decrease to the end of the experiment with an ORP of ≈ -616 mV. The ORP for the GFH1 treatment is above the control at the first hour sampling point with an ORP of ≈ -426 mV. The ORP decreases to above the control at hour 360 with an ORP of ≈ -591 mV and stabilizes for the remainder of

the experiment. The ORP for the GFH2 treatment is above the control until the 6-hour sampling point with an ORP of ≈ -515 mV. The ORP remains the same as the control to the end of the experiment.

#### 2.3.3.2 Re sorption

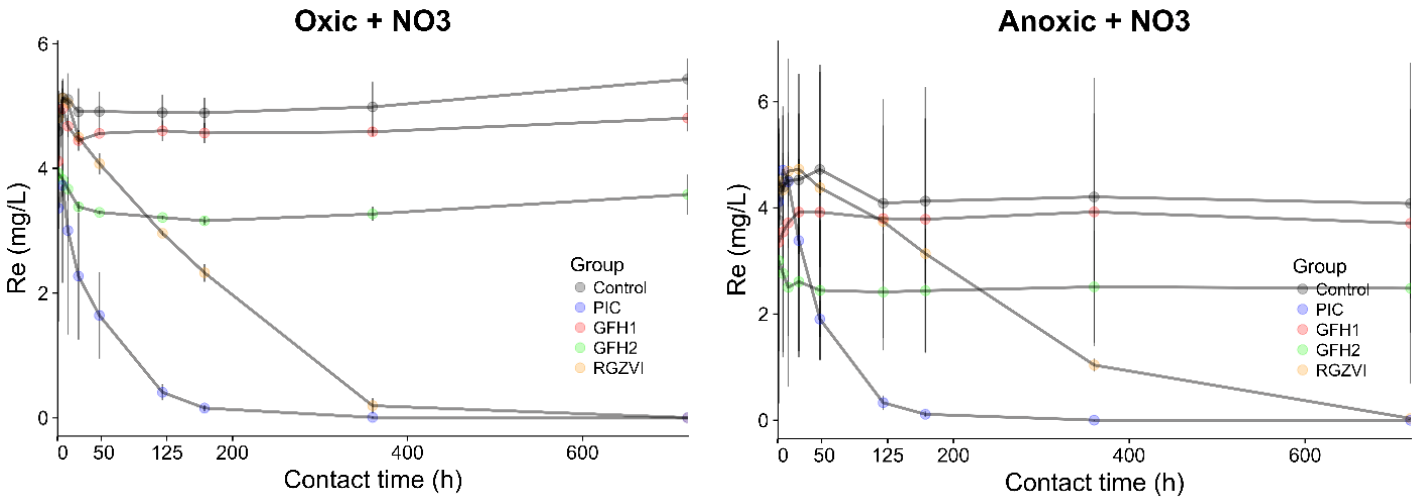


*(a)* *(b)*

*Figure 2.8: Rhenium in solution containing $NO_3^-$ in the oxic (a) and anoxic (b) test condition, shown with 95% confidence intervals.*

In general, there was more variation in the Re sorption results for the treatments containing $NO_3^-$. However, the trends with respect to Re removal from solution are generally consistent with those demonstrated in Figure 2.3, with PIC being the most effective followed

by ZVI. Figure 2.8 shows the Re concentration (in mg $L^{-1}$) versus the contact time (in hours) for the no sorbent control, PIC, ZVI, GFH1, and GFH2 treatments in the oxic (a) and anoxic (b) environment. Under oxic conditions (Fig. 2a), the Re concentration in the control batch starts at 4.59± 0.05 mg $L^{-1}$ and does not change for the reminder of the equilibration time. For the PIC treatment, the Re concentration stays the same as the control until hour 12 when the concentration is 3.00 ± 1.66 mg $L^{-1}$ and decreases at hour 120 when the concentration is 0.40 ± 0.13 mg $L^{-1}$. The Re concentration is below detection at hour 168. For the ZVI the Re concentration stays the same as the control until the 48-hour sampling with a concentration of 4.07 ± 0.17 mg $L^{-1}$. The concentration then decreases significantly until it is no longer detectable by the 360-hour sampling event. For the GFH1 treatment the Re concentration is the same as that of the control through the entire experiment. The Re concentration for the GFH2 is the same as the control until the 6-hour sampling event when the concentration is 3.18 ± 0.26 mg $L^{-1}$. The concentration decreases to reach 3.38 ± 0.08 mg $L^{-1}$ at hour 24, then continues to decrease to 3.21 ± 0.03 mg $L^{-1}$ at hour 120 and remains stable till the end of the experiment.

Under anoxic conditions (Fig. 2b), the Re concentration for the no sorbent control batch is initially 3.76 ± 1.04 mg $L^{-1}$ and remains the same throughout the experiment. For the PIC treatment, the Re concentration is the same as the control until the 48-hour sampling event when the concentration is 1.90 ± 0.34 mg $L^{-1}$. The concentration decreases until it is no longer detectable at hour 360. For the ZVI treatment, the Re concentration was the same as the control until the 360-hour sampling event when the concentration was 1.03 ± 0.11 mg $L^{-1}$. The Re concentration continued to decrease, reaching 0.03 ± 0.01 mg $L^{-1}$ at hour 720. The Re

concentration for the GFH1 and GFH2 treatments were the same as the control throughout the experiment.

#### 2.3.3.3 Nitrate sorption

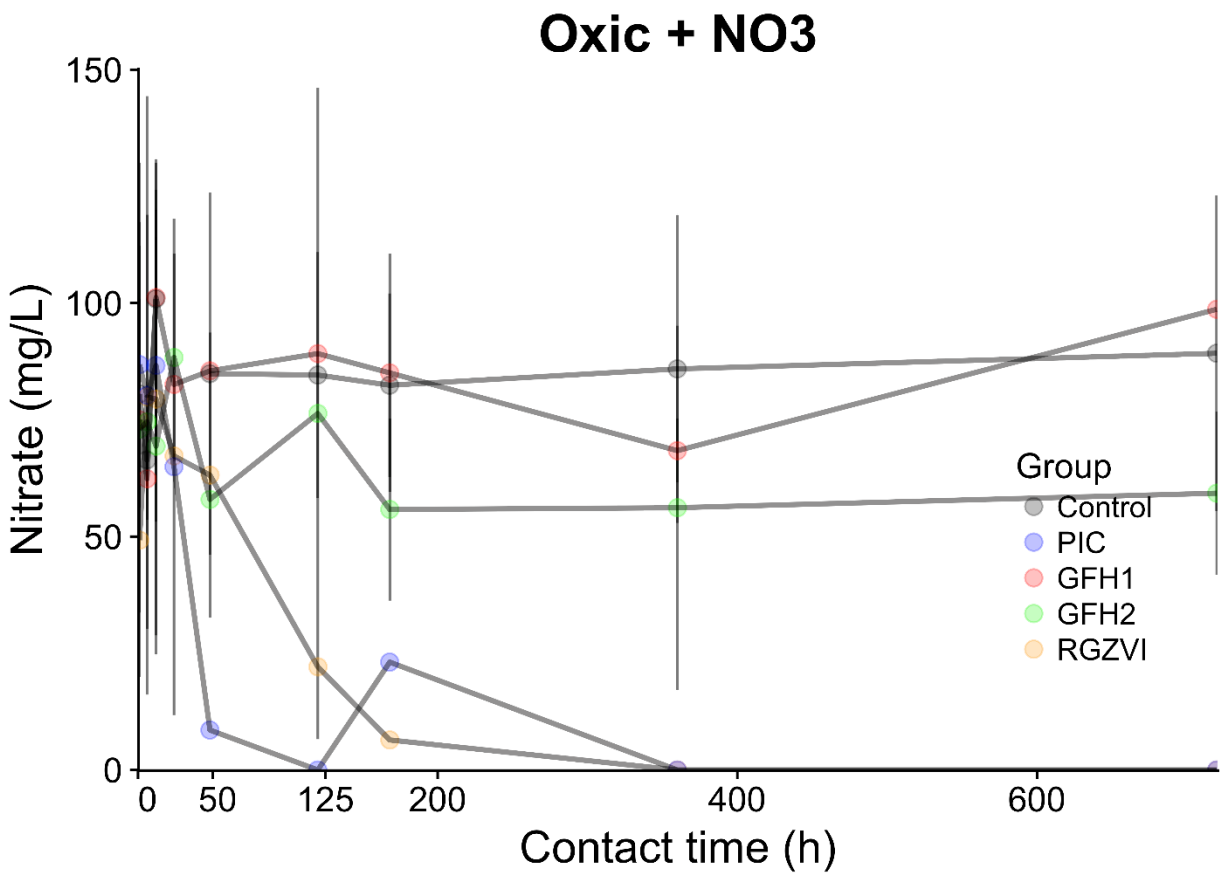


*Figure 2.9: Residual $NO_3^-$ in solution in the oxic (a) and anoxic (b) treatment atmospheres*

Figure 2.9 shows the nitrate ($NO_3^-$) concentration (in mg $L^{-1}$) versus time (in hours) for the control, PIC, ZVI, GFH1, and GFH2 treatments in the oxic test environment. While there

is considerable scatter in the data, only the PIC and ZVI treatments display clear reductions in $NO_3^-$ over the course of the experiment. Under oxic conditions, the $NO_3^-$ concentration in the control was initially 80.5 ± 12.8 mg $L^{-1}$ which remains stable throughout the experiment. The $NO_3^-$ concentration in the PIC treatment was the same as the control until the 48-hour sampling time when the concentration went below the control concentration reaching 8.55 ± 14.81 mg $L^{-1}$. Nitrate was no longer detectable in the 120-hour sampling point. Due to analytical error, the $NO_3^-$ concentration appeared to be 0.00 mg $L^{-1}$ within error, however at the next sampling time, the concentration was below the detection limit again. The $NO_3^-$ concentration in the solution of the ZVI treatment stayed the same as the control until the 120-hour sampling point when it fell below the control with a concentration of 22.09 ± 0.05 mg $L^{-1}$. At the 360-hour sampling event, the $NO_3^-$ concentration for the ZVI treatment was below the detection limit. The $NO_3^-$ concentration in the GFH1 solution remained the same as the control concentration throughout the experiment. The $NO_3^-$ concentration in the GFH2 solution stayed the same as the control until the 168-hour sampling point as it went below the control with a concentration of 55.8 ± 7.9 mg $L^{-1}$ and stayed below the control concentration to the end of the experiment. The residual $NO_3^-$ graph for the anoxic test environment was not shown as the results were consistent to the oxic test environment, with significant decreases in detectable $NO_3^-$ largely restricted to the PIC and ZVI treatments.

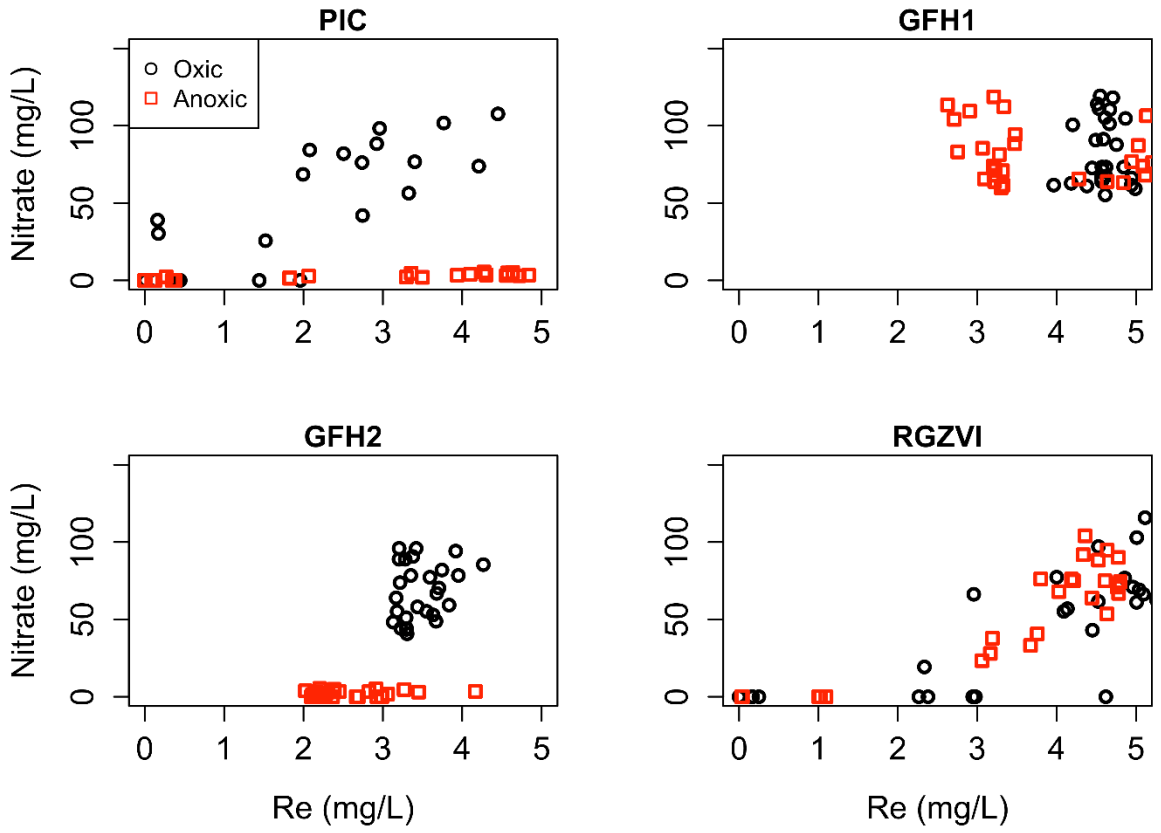


*Figure 2.10: Linear regression comparing $NO_3^-$ in solution to Re in solution to test for correlation in the in the oxic and anoxic test environments*

Linear regression was carried out on the batch experiment data to determine if there were any correlations between $NO_3^-$ concentration and Re concentration in solution in both test environments, oxic and anoxic. The results, Figure 2.10, determined there was no significant correlation between the two.

*Table 2.4: Residual Fe in treatment solutions with $NO_3^-$ in the oxic and anoxic environments*

| Treatment | Oxic Fe (mg/L) | Anoxic Fe (mg/L) |
|---|---|---|
| **PIC** | 2.10 | 9.85 |
| **ZVI** | 0.51 | 0.89 |
| **GFH1** | 4.88 | 0.57 |
| **GFH2** | 49.68 | 94.00 |

Table 2.4 shows the total amount of Fe collected from the treatment solutions with $NO_3^-$ in both the oxic and anoxic environments. The no sorbent control treatment is not shown for obvious reasons. Each treatment released some Fe into the solution, however, the GFH2 treatment released the most Iron (as colloidal or nanoparticulate) ≈ 49.9 mg $L^{-1}$ and 94.0 mg $L^{-1}$ for the oxic and anoxic, respectively.

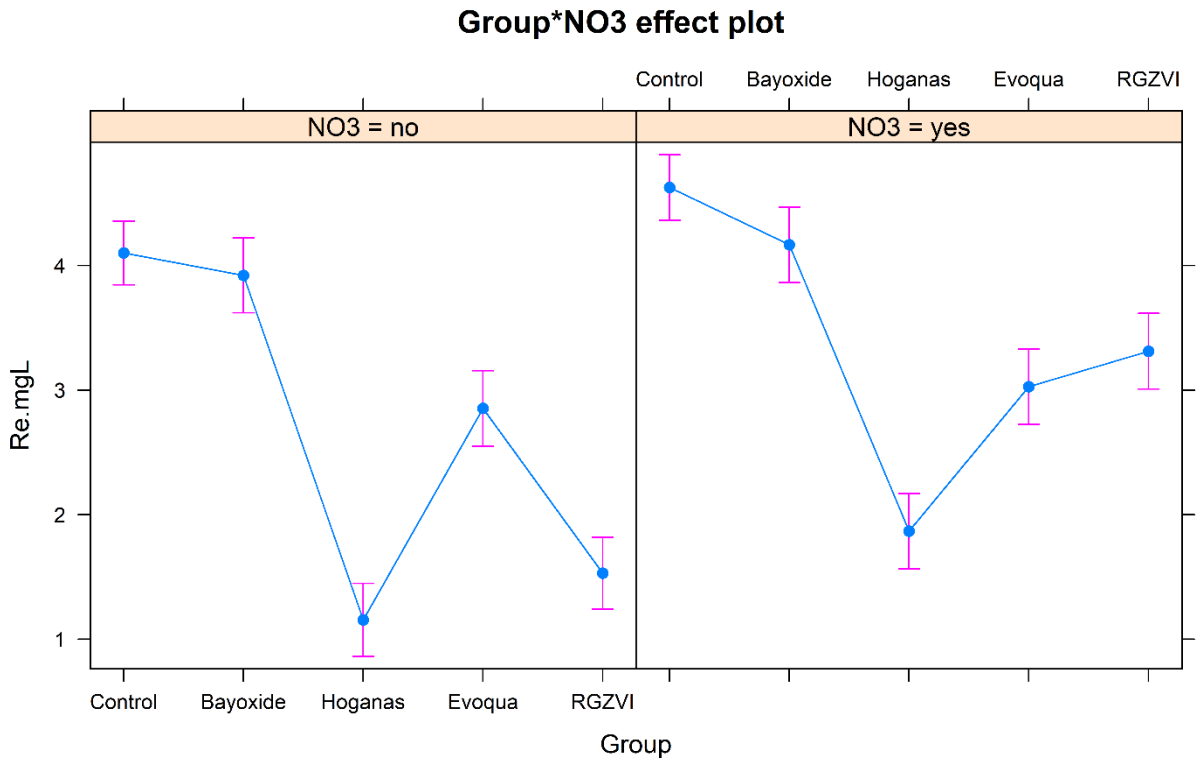


*Figure 2.11: Results from Tukey multiple comparison of means on the Re concentrations in the presence and absence of $NO_3^-$*

#### 2.3.3.4 Statistical effect of Nitrate on Re immobilization

A Tukey multiple comparison of means test was carried out to determine if there was a significant difference in Re concentration of all groups (i.e., PIC, ZVI, GFH1, and GFH2) in the presence and absence of $NO_3$ with a 95% confidence level. The results, Figure 2.11, show there is a significant difference between Re concentrations with and without nitrate only for the ZVI. The Re sorption on the PIC materials is not influenced by the presence of nitrate in solution.

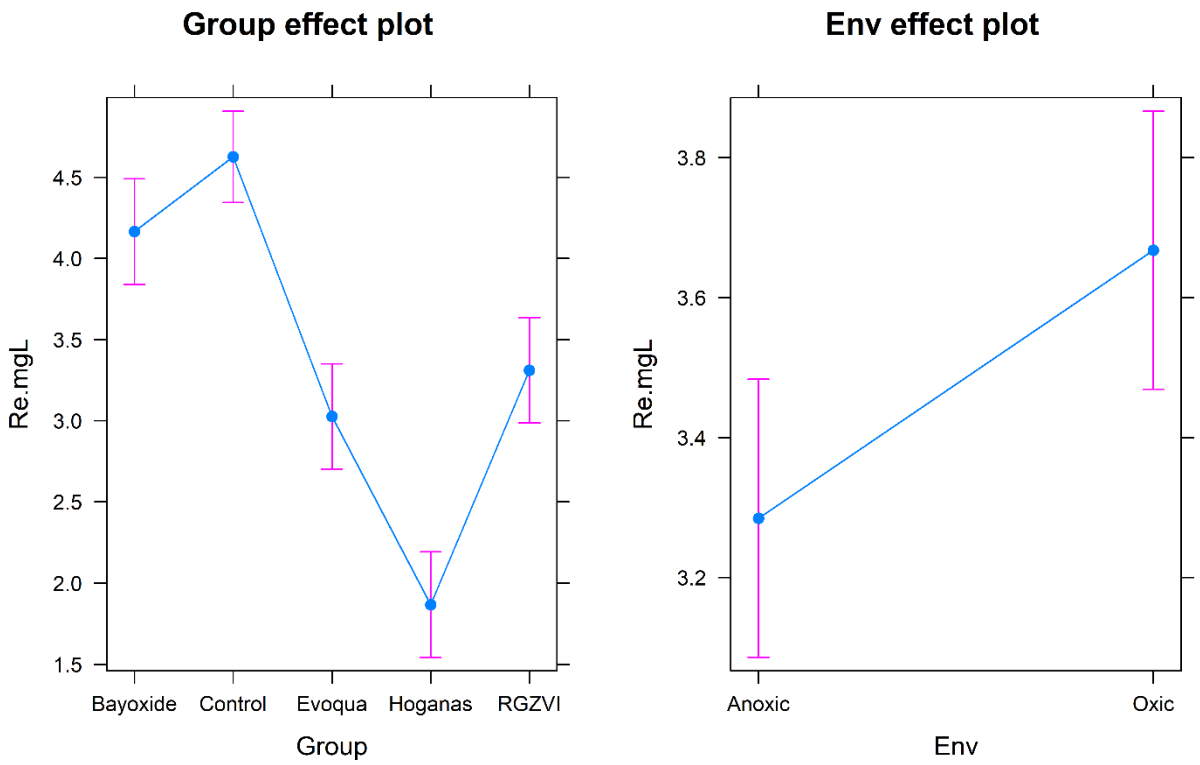


*Figure 2.12: Results of an ANOVA test comparing the mean Re concentrations of all groups to the Re concentration in the control for experiments in the presence of $NO_3^-$*

Table 2.5: *Computer output of ANOVA test comparing the mean Re concentrations of all groups to the Re concentration in the control for experiments in the presence of $NO_3^-$*

| | **Estimated** | **Std. Error** | **t value** | **Pr(>\|t\|)** |
|---|---|---|---|---|
| **(Intercept)** | 3.97 | 0.18 | 22.1 | 2e-16 |
| **Control** | 0.46 | 0.22 | 2.11 | 0.04 |
| **GFH2** | -1.14 | 0.23 | -4.89 | 1.7e-06 |
| **PIC** | -2.30 | 0.23 | -9.86 | <2e-16 |
| **ZVI** | -0.85 | 0.23 | -3.67 | 0.00 |
| **Oxic** | 0.38 | 0.14 | 2.68 | 0.01 |

Since there was no significant effect of the environment on the Re concentration, an analysis of variance (ANOVA) test was run to compare the mean concentration of Re of all the groups to the control in the presence of $NO_3$. The results are presented in Table 2.5 and Figure 2.12. The predicted Re concentration in the no sorbent control is 3.97 ± 0.18 mg $L^{-1,}$ which is the baseline. The Re concentration in the no sorbent control is 0.46 ± 0.22 mg $L^{-1}$ above the baseline, this is not a significant difference; Pr(>|t|)0.04<0.05. The Re concentration in the GFH2 group is 1.14 ± 0.23 mg $L^{-1}$ below the baseline, this is a significant difference; Pr(>|t|)<1.7e-06<<0.05. The Re concentration for the PIC group is 2.30 ± 0.23 mg $L^{-1}$ below the baseline, this is a significant difference; Pr(>|t|)<2e-16<<<<0.05. The Re concentration for ZVI is 0.85 ± 0.23 mg $L^{-1}$ below the baseline, this is a significant difference; Pr(>|t|) 0.00<0.05. The mean Re concentration of the oxic environment is 0.38 ± 0.14 mg $L^{-1}$ above the baseline, this difference is significant; Pr(>|t|)0.01<0.05.

## 2.4 Discussion

### 2.4.1 Rhenium sorption by iron materials

The PIC and ZVI completely removed Re from the solution in both the oxic and anoxic environments (Figure 2.3 (a) and (b)). The PIC performed best by completely removing the Re within the first 168 hours of equilibration. The ZVI took slightly longer to completely remove the Re from the solution, which was roughly 15 days in the oxic environment, while surprisingly leaving some residual $Re_{(aq)}$ in the anoxic environment. The GFH1 and GFH2 treatments showed some limited Re sorption capacity that appeared transient at best. Notably the Re concentration initially decreased for the first five days, but increased for the remaining

equilibration time, the mechanism for which is unclear. As supported by XRD analysis, the PIC and the ZVI largely contain zero-valent iron while GFH1 and GFH2 are comprised of iron(oxy)hydroxides. As the zero-valent iron as a strong reduction capacity, this suggests that the reduction of Re plays a significant role in the sorption reaction for PIC and ZVI.

### 2.4.2 Effect of the presence of zero-valent iron in iron material

For the PIC and the ZVI materials, it is interesting to note that the removal of Re from solution in the anoxic atmosphere is quite similar for each sorbent treatment to that of the oxic atmosphere, which was open to the laboratory environment. One expects Re sorption associated with chemical reduction due to $Fe^0$ to be more rapid in the absence of dissolved $O_2$. However, such a trend is not evident in the current results, and the ANOVA test further confirms that the test atmosphere did not have an effect on Re sorption.

As discussed above, the PIC material was the best Re sorbent regardless of the test atmosphere in the presence and absence of $NO_3^-$, with the ZVI treatment being the next best sorbent. The two Fe oxide materials, GFH1 and GFH2, display very limited capacity to sorb Re in either atmosphere.

There were very few differences between the oxic and anoxic environments in terms of Re sorption and $NO_3^-$ removal; thus it appears that the presence of $O_2$ does not interfere with Re sorption under the present conditions. However, the scatter observed with respect to ORP and pH for oxic treatments indicate that there may be some degree of reaction gradients within the equilibrating vessels that were open to the lab atmosphere for the PIC and ZVI treatments.

The pH in each treatment displaying Re sorption (Figures 2.2 and 2.7) initially increases then plateaus as the experiment continues. This is consistent with the reduction reaction (eq. 2.1) for $ReO_4^-$ (Re(VII)) to $ReO_{2(s)}$ (Re(IV)), as it consumes $H^+$ ions resulting in an increase in the pH for the solution.

$$ReO_{4(aq)}^- + 4H^+ + 3e^- \rightarrow ReO_{2(s)} + 2H_2O_{(l)} \quad Eq.\,2.1$$

Lenell et al. (2017) reported that $ReO_4^-$ sorption by ZVI is highest at near neutral pH (pH = 7) and that sorption was inhibited under alkaline conditions (Lenell and Arai, 2017). However, the newly dissolved ferrous species (i.e., Fe(II)) can further react with $^-OH$ that is present in solution to form ferrous hydroxides (green rust) as corrosion products (Zhou et al., 2014). This can further oxidize to form mixed-valence Fe oxide species, such as magnetite ($Fe_3O_4$).

Under certain conditions, ZVI in a $Fe^0/H_2O$ system will undergo a series of reactions resulting in various corrosion products as the Fe is oxidized. XRD analysis shows that the PIC material initially contains a small amount of $Fe_3O_4$ (Fig. A.1); however, the amount of Fe-oxides increases with continued reaction in the aqueous system (Figs. A.2 and A.2). Figure A.5 is the XRD pattern for the initial ZVI material, displaying only the peaks associated with $Fe^0$. With equilibration in an aqueous system the corrosion products (e.g., $Fe_3O_4$) becomes evident (Figs A.6 and A.7).

On the PIC materials, the newly formed $Fe_3O_4$ species may also sorb $ReO_4^-$, which can become entrapped in its structure, providing another mechanism for $ReO_4^-$ removal from the bulk solution (Guan et al., 2015).

The reduction of $NO_3^-$ by ZVI and PIC also consumes acidity, with multiple nitrogen products possible depending on the exact chemical condition (Eqs. 2.2 and 2.3):

$$Fe^0_{(s)} + NO^-_{3(aq)} + 9H^+_{(aq)} \rightarrow 4Fe^+_{(aq)} + NH_{3(aq)} + 3H_2O_{(l)} \qquad Eq.2.2$$

$$5Fe^0_{(s)} + 2NO^-_{3(aq)} + 12H^+_{(aq)} \rightarrow 5Fe^{2+}_{(aq)} + N_2 + 6H_2O_{(l)} \qquad Eq.2.3$$

However, Zhang et al. (2017) assert that the production of $NH_3^+$ in this system is more thermodynamically favorable than the production of $N_2$, consistent with our observations (Zhang et al., 2017).

Once again the PIC treatment did the best in both the oxic and anoxic environments at removing Re and $NO_3^-$ from solution. The PIC took slightly longer to remove the Re from the solution in the presence of $NO_3^-$ than in the absence of $NO_3^-$. The Re in the presence of nitrate was completely removed by the 15-day sample event, where without nitrate the Re was removed by the 7-day sample event. The ZVI performed the second best; however, 0.03 mg $L^{-1}$ Re remained in the solution at the end of the equilibration. When $NO_3^-$ was not present, the ZVI completely removed the Re but took longer to do so than the PIC.

### 2.4.3 Nitrate Immobilization

The PIC material performed best at removing the $NO_3^-$ from solution in both the oxic and anoxic environments. Under oxic conditions, $NO_3^-$ was completely removed within the first 5 days, which was faster than the removal of Re. Under the anoxic environment the $NO_3^-$ was completely removed within the first 7 days, which was also faster than the removal of $ReO_4^-$. These results are consistent with the standard redox potentials for $NO_3^-$ ($E^0 = 0.88$) and $ReO_4^-$

($E^0$ = -0.55), with the more positive potential associated with $NO_3^-$ having the higher affinity for available electrons. However, from the ANOVA comparing the differences in Re concentrations when $NO_3^-$ was present and absent, it was determined that for the PIC treatment, in the presence $NO_3^-$ Re sorption is not affected.

When $NO_3^-$ is reduced, the reduction products can either be $N_2$, which may degas from solution, or $NH_3$. At pH 9.25 half of the ammonia will be un-ionized ($NH_3$) and half will be ammonium ($NH_4^+$), (i.e., $NH_4^+$ $pK_a$ = 9.25 at 25°C). As the pH increases so does the volatility of the $NH_3$ species (Mitra et al., 2011).

# CHAPTER 3

# IMMOBILIZATION OF RHENIUM AS A TECHNETIUM ANALOGUE USING IRON MATERIALS IN COLUMN EXPERIMENTS

## 3.1 Introduction

Groundwater resources are highly vulnerable to contamination if not managed properly (Dillon et al., 2000). There are many reports of serious incidents of groundwater contamination due to accidental spills, or unsatisfactory disposal of industrial chemicals, agricultural practices, mining activities, etc. The U.S. Environmental Protection Agency (US EPA) reported that large-scale groundwater cleanup began in the 1980s but rarely produced the expected reduction in contamination levels (US, 1989). One of the most promising remediation technologies is the permeable reactive barrier (PRB). The PRB method utilizes a strategically placed passive permeable treatment wall filled with reactive materials, which is installed in the path of a contaminated groundwater plume. This remediation strategy is quite similar to the utilization of reactive sorbents in an above-ground filter system for the treatment of process waste water prior to discharge or the selective removal of contaminants from municipal groundwater systems.

When passing through the wall, contaminants in the groundwater can be removed by degradation, precipitation and sorption processes due to physical, chemical, biochemical or integrated interactions between the target contaminants and reactive materials

(Thiruvenkatachari et al., 2008, Weber et al., 2013, Wantanaphong et al., 2006, Ruhl et al., 2012, Zhou et al., 2014).

Materials commonly used for PRB systems include zero-valent iron (ZVI), activated carbon (AC) (Rijnaarts et al., 1997), zeolite (Kovalick and Kingscott, 1995), and peat (Yang, 2000). The most widely utilized of these materials, in both laboratory studies and field applications, is ZVI (Gavaskar et al., 1998).

ZVI has a high reductive capacity, -440 mV, and acts primarily as a reductant in most systems, transferring electrons to the contaminants while becoming oxidized (Meggyes and Simon, 2000). ZVI has been shown to be effective at immobilizing certain toxic metals (Cr, Mn, Ni, Pb, Cu, Zn, etc.) (Blowes et al., 2000), radionuclides (U, Pu) (Xiang et al., 2018, Chen et al., 2017, Crane et al., 2015), and nitrate (Gandhi et al., 2002), while also degrading petroleum hydrocarbons and halogenated organic compounds (Guerin et al., 2002).

The use of ZVI alone as the reactive medium has limitations with respect to the long-term hydraulic properties and removal efficiency due to the deactivation associated with the buildup of corrosion products that also clog barrier pores (Liang et al., 2005, Li et al., 2006, Ruhl et al., 2012). Most important to note, iron corrosion increases the pH inside iron PRBs and promotes precipitation of secondary minerals which can affect the longevity of the PRBs (Carniato et al., 2012).

Under environmental conditions, ZVI is unstable and undergoes a series of corrosion reactions in $Fe^0/H_2O$ system. The oxidation of $Fe^0$ by $H^+/O_2$ yields $Fe^{2+}$ (Eq. 3.1 and 3.2) (Noubactep, 2008).

$$Fe^0 + 2H^+ \rightarrow Fe^{2+} + H_2 \qquad Eq.3.1$$

$$2Fe^0 + O_2 + 2H_2O \rightarrow 2Fe^{2+} + 4OH^- \qquad Eq.3.2$$

In the pH range of natural waters, $Fe^{2+}$ may hydrolyze and form $Fe(OH)_2$ at the $Fe^0$ surface (Eq. 3.3). The further oxidation of $Fe^{2+}$ species by $O_2$ is quite rapid with the reaction rate increasing with increasing pH (Guan et al., 2011, Aleksanyan et al., 2007, Nešić, 2007).

$$4Fe^{2+} + 4H^+ + O_2 \rightarrow 4Fe^{3+} + 2H_2O \qquad Eq.3.3$$

The resulting $Fe^{3+}$ readily hydrolyzes and precipitates, and depending on $O_2$ availability, various (hydr)oxides are generated (Mackenzie et al., 1999, Mielczarski et al., 2005, Wilkin et al., 2003).

$$Fe^{3+} + 3H_2O \rightarrow Fe(OH)_{3(s)} + 3H^+ \qquad Eq.3.4$$

Therefore, in oxygenated waters, a thicker layer of Fe(III) oxides (oxidized passivation layer) will form on the outer surface, decreasing the reactivity of ZVI (Flury et al., 2009). As this passivation layer forms, it may also clog the matrix pores, resulting in a decrease in the hydraulic conductivity of the reactive barrier system. While the precipitation of Fe(III) oxy-hydroxides may generate acidity, the ZVI corrosion process tends to consume $H^+$ ions, which increases the pH of the system and further decreases ZVI reactivity (Guan et al., 2015).

The objective of this study was to evaluate the effectiveness of a novel porous iron composite (PIC) material for use as a permeable reactive barrier or a filter for the removal of technetium-99 ($^{99}Tc$), as the highly mobile oxidized pertechnetate species (i.e., $TcO_4^-{}_{(aq)}$), from contaminated groundwater/process water in the presence of other competing oxidized

reactive species (i.e., $NO_3^-$ and $O_2$), that are likely to be present in much higher concentrations. In the current study, Re(VII) as perrhenate ($ReO_4^-{}_{(aq)}$) was used as a non-radioactive analog for Tc(VII). The new PIC material, produced via a proprietary process, is essentially a modified, high surface area, highly reactive form of ZVI (Hu, 2016). Previous laboratory batch experiments discussed in Chapter 2 demonstrated the ability of the PIC material to more effectively immobilize Re(VII) (i.e., Tc(VII)) when compared to conventional ZVI and other Fe-oxide based commercial sorbents. To accomplish the current objective, laboratory column tests were carried out using PIC material to assess its ability to immobilize Re from solution in the presence and absence of $NO_3^-$, an alternative electron acceptor in contaminated groundwater.

### 3.2 Materials and Methods

Four column experiments were conducted using Re as a surrogate for Tc: 1) a control test using sand as a non-reactive (limited) sorbent; 2) a Re breakthrough test using the PIC sorbent material; 3) a Re breakthrough test using the PIC material with $NO_3^-$ also present in the inlet solution, and 4) a Re breakthrough test using an Artificial Groundwater (AGW) surrogate that does not contain $NO_3^-$ (Cf. Table 2.1). No effort was taken to restrict the exposure to dissolved $O_2$ as all of the inlet test solutions were open to the laboratory atmosphere.

### 3.2.1 Stock solutions

Stock solutions of $NaReO_4$ were made by dissolving 0.22 g $NaReO_{4(s)}$ in 1 L of milliq water resulting in a 150 ppm solution of $Re_{(aq)}$. A stock NaCl solution was made by dissolving 58.4 g $NaCl_{(s)}$ in 1 L milliQ water, resulting in a 1 M NaCl solution. A 1 M $NO_3^-$ solution was by dissolving 42.50 g $NaNO_{3(s)}$ in a 500-mL volumetric flask brought to volume using milliQ water.

The stock solution of 4 ppm Re (Cf. Rhenium solution Table 1-1) was made by mixing 53 mL of 150 ppm $Re_{(aq)}$ with 20.00 mL 1 M NaCl in a 2,000-mL volumetric flask, the flask was brought to volume using milliQ water.

For the solution of 4 ppm Re and 100 ppm $NO_3^-$ (Cf. Nitrate Solution Table 2.1) 53 mL of the 150 ppm Re, 2.35 mL of the 1.0M $NaNO_3$, and 17.65 mL of the 1.0M $NaCl_{(l)}$ were mixed together in a 2 L volumetric flask brought to volume with milliQ water.

For the solution of AGW, 53 mL of the 150 ppm Re and 2.00 mL of the AGW stock solution were mixed together in a 2 L volumetric flask brought to volume with milliQ water.

*Table 3.1: Final compositions of column treatment solutions*

| | Rhenium Solution | Rhenium + Nitrate Solution | Artificial Groundwater Solution (AGW) |
|---|---|---|---|
| Re (mg $L^{-1}$) | 4.00 | 4 | 4 |
| $NO_3$ (mg $L^{-1}$) | | 100.00 | |
| Na (mg $L^{-1}$) | 230.4 | 230.4 | 1.88 |
| Cl (mg $L^{-1}$) | 354.5 | 312.9 | 5.51 |
| Mg (mg $L^{-1}$) | | | 0.66 |
| Ca (mg $L^{-1}$) | | | 1.00 |
| K (mg $L^{-1}$) | | | 0.21 |
| $SO_4$ (mg $L^{-1}$) | | | 0.73 |

### 3.2.2 Material

The reactive sorbent material was a Porous Iron Composite (PIC) material developed by North American Höganäs, Inc. (Cf. Chapter 2).

### 3.2.3 Column set-up

The laboratory column system was designed to mimic conventional flow-through filter applications. Clear polyvinyl chloride (PVC) tubing with an inner diameter of 2.66 cm and a length of 8 cm was used for the filter column. Plastic mesh was placed at the inlet and outlet of the column to retain the reactive materials. For the PIC tests, the filter column was packed with 30 g of Ottawa sand at the bottom followed by 50 g PIC material, then another 30 g of Ottawa sand on the top to hold the reactive material in place and better disperse flow across the cross section of the reactive filter material. An additional filter column containing only 110 g of sand was evaluated as an experimental control. A peristaltic pump was used to maintain a constant, controlled inlet flow rate. A flow through pH electrode was placed at the

column outlet to monitor the pH of the effluent, and a fraction collector was used to collect effluent samples for additional chemical analysis.

### 3.2.4 Column experiments

Before the treatment solutions were leached through the column, 0.01 M $NaCl_{(l)}$ was initially used to saturate the columns for three hours. The appropriate treatment solution (Table 3.1) was then leached through separate columns at a flow rate of 1 mL $min^{-1}$, and effluent samples were collected for chemical analysis. Filter plugging, as influenced by solution treatment, was monitored using a piezometer tube at the column inlet, with head buildup monitored periodically throughout testing. The effluent samples were filtered (0.2µm pore-size filter) and acidified (2% $HNO_3$) for preservation in preparation for analysis of Re, Fe, Na, calcium (Ca), aluminum (Al), magnesium (Mg), and potassium (K) using inductively coupled-plasma mass spectrometry (ICP-MS) on a Nexlon 300 (Perkin Elmer, Inc.) in accordance with the quality assurance (QA) and quality control (QC) protocols of EPA method 6020A (USEPA, 2007a). Other important reactive solution components were analyzed as follows: $NO_3^-$ was determined by the Chromotropic Acid test method, $NO_2^-$ was determined by the Diazotization method (APHA 1997b), and $NH_4^+/NH_3$ was determined by the Phenate method (APHA 1997a).


*Figure 3.1: Image of the experimental column system with flow in an upward direction*

### 3.2.5 Liquid-solid ratio

The Liquid-Solid ratio represents the amount of liquid in L, that went through the material in Kg (of dry material). The liquid-solid ratio (L/S) was used to provide a reasonable means of comparing the results of various column treatments.

## 3.3 Results

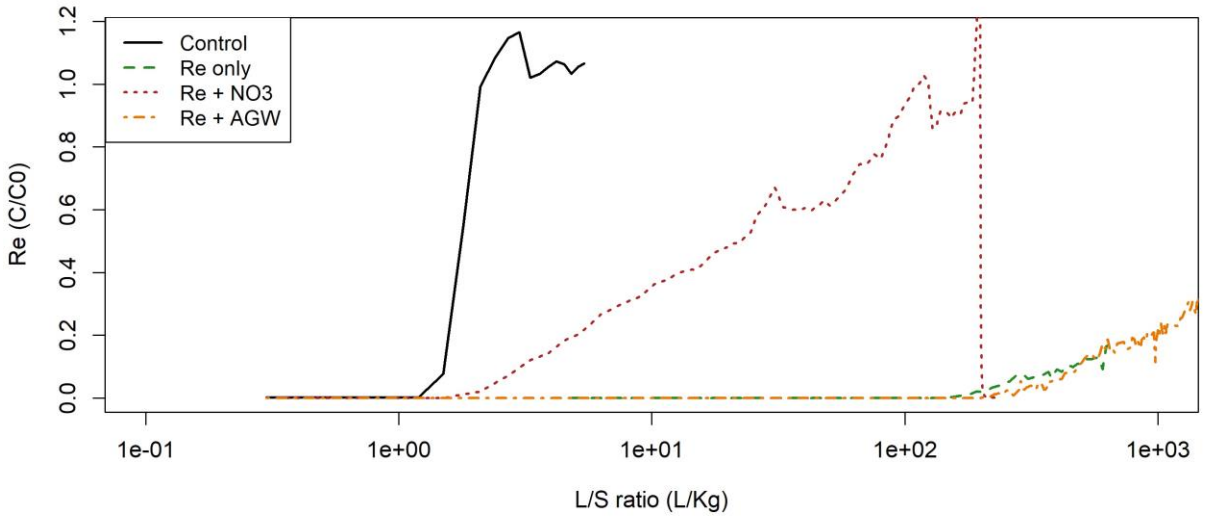


*Figure 3.2: Ratio of Re concentration in the column effluent (C) to the Re concentration in column influent ($C_0$) over the liquid to solid ratio of the column*

The effluent Re concentration (i.e., $C/C_0$) as a function of the inlet concentration (i.e., $C_0 \approx 4$ mg $L^{-1}$) for the various column treatments in presented in Figure 3.2. All column tests were conducted at a constant inlet flow rate of 1 mL $min^{-1}$. The effluent Re breakthrough

data are presented in terms of the liquid to initial solid ratio i.e., mL of filtrate divided by mass of PIC; L/S), with results presented on a logarithmic scale because of the extended treatment durations for some of the column tests. Rhenium breakthrough for the control column (i.e., sand) was quite rapid, with full breakthrough occurring at ~ 2.4 L $Kg^{-1}$s. Full Re breakthrough was never observed for the PIC material in the absence of the competing oxidant (i.e., $NO_3^-$) despite the extended leaching duration (1,509 hrs; 90+ L). Limited initial Re breakthrough was detected at around ≈149 L $Kg^{-1}$, and Re slowly increased with continued leaching for a final effluent concentration that reached approximately 1 mg $L^{-1}$ around ≈ 624 L $Kg^{-1}$. Rhenium breakthrough in the AGW solution was somewhat similar to that of the Re-only leaching test, if even a bit more delayed due to the lower ionic strength of the leaching solution, with Re in the effluent becoming detectable at ≈ 208 L $Kg^{-1}$. The Re slowly increased reaching ≈ 1.0 mg $L^{-1}$ around ≈ 906 L $Kg^{-1}$. This is not surprising since the AGW leaching solution did not include any alternate oxidants, like $NO_3^-$, that might compete with Re(VII) for the PIC sorption capacity. In contrast to the Re only and Re-AGW results for the PIC materials, Re breakthrough in the presence of $NO_3^-$ was achieved around ≈ 114 L $Kg^{-1}$. For the Re-$NO_3^-$ treatment, breakthrough was achieved showing that the presence of $NO_3^-$ has an effect on the immobilization of Re in the column. For the Re only and Re-AGW treatment, the PIC material was able to immobilize more Re than the Re-$NO_3^-$ treatment.

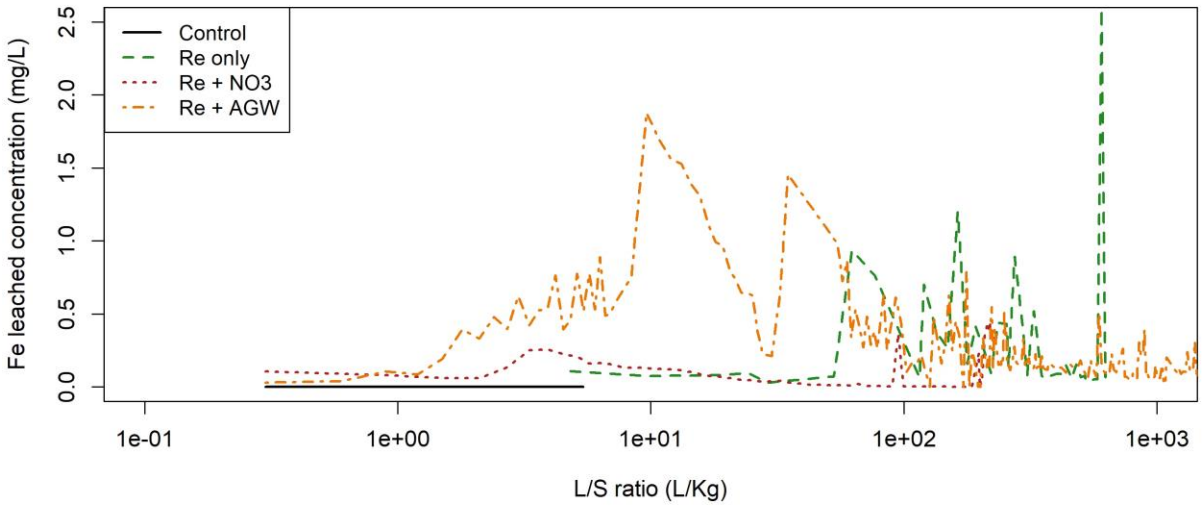


*Figure 3.3: Concentration of Fe leached from the column over the liquid to solid ratio of the column for each treatment*

Soluble Fe present in the column effluent for each leachate treatment is shown in Figure 3.3. As expected, no soluble Fe was detected in the effluent for the control treatment using sand as the filter material. Only limited dissolved Fe was detected in the Re with $NO_3^-$ leachate treatment at the time when Re first becomes detectable in the effluent despite the clear evidence of Re immobilization and $NO_3^-$ reduction associated with the responsible Fe reactions. The lack of significant Fe in the effluent is presumably caused by the presence of $NO_3^-$ which serves as an additional oxidant to ensure more complete Fe oxidation and precipitation as Fe oxy-hydroxides within the filter matrix. For the Re leachates with $NO_3^-$, generally higher effluent Fe concentrations were observed. However, the effluent Fe concentrations appear to oscillate in a somewhat predictable manner, with the oscillations apparently shortening over time due to the logarithmic nature of the x-axis in Figure 3.3. This

pattern is likely an artifact associated with how the samples were collected, filtered and then acidified for chemical analysis, with higher levels of dissolved Fe observed for samples that were immediately filtered and acidified for subsequent analysis as the samples were collected. In contrast, the level of soluble Fe clearly decreased if the effluent samples oxidized and Fe(III) precipitated with storage before filtration and acidification for analysis.

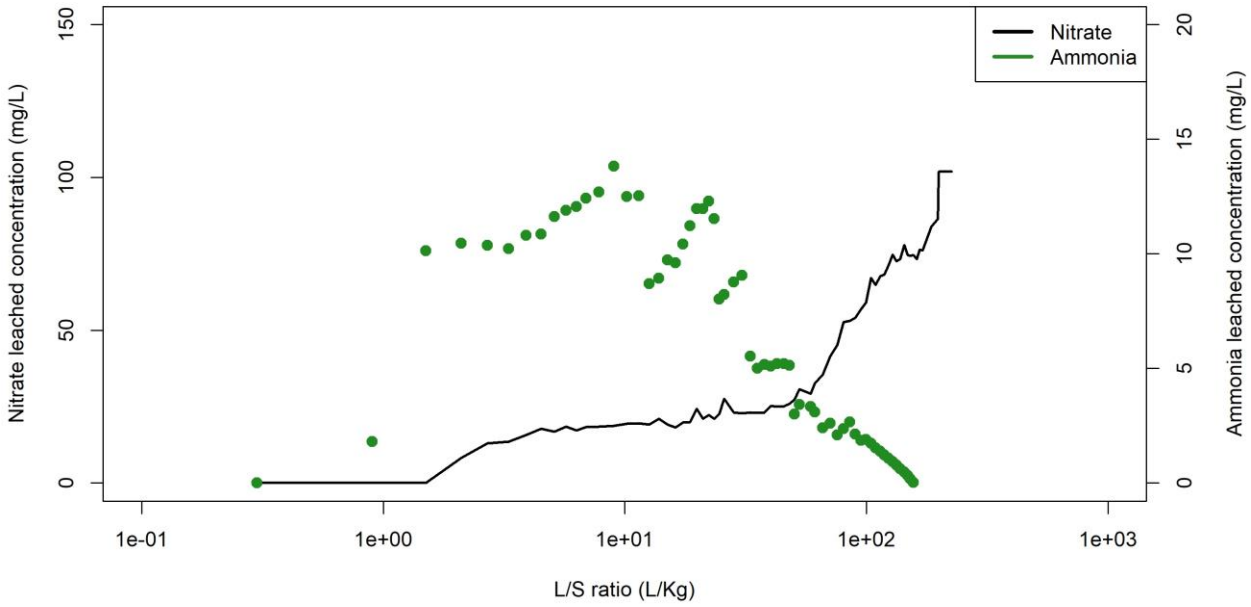


*Figure 3.4: Nitrate and ammonia in column effluent for the Re + $NO_3^-$ treatment*

The $NO_3^-$ and $NH_3/NH_4^+$ concentrations in the column effluent for the Re + $NO_3^-$ leachate treatment are shown in Figure 3.4. Little or no detectable nitrite ($NO_2^-$) was ever present in the column effluent. Limited $NO_3^-$ is initially detected in the column effluent, but it increases to ≈ 0.21 mg $L^{-1}$ at around 7.8 L $Kg^{-1}$. The presence of detectable $NH_3/NH_4^+$ in the effluent occurs just before detection of any $NO_3^-$ and increases quickly to ≈ 10.1 mg $L^{-1}$ at 1.25 L $Kg^-$

$^{1}$, and then remains between 9 to 14 mg $L^{-1}$ through 20.5 L $Kg^{-1}$, with limited $NO_3^-$ present in the effluent. The $NH_3/NH_4^+$ begins to dramatically decrease just before the level of $NO_3^-$ in the effluent clearly increases, approaching the same concentration as the inlet treatment solution.

The reduction of $NO_3^-$ by ZVI proceeds according to the following reaction, with multiple nitrogen products possible depending on the exact chemical conditions. However, the production of $NH_3$ is more thermodynamically favorable than $N_2$ (Zhang et al., 2017).

$$4Fe^0_{(s)} + NO^-_{3(aq)} + 9H^+_{(aq)} \rightarrow 4Fe^{2+}_{(aq)} + NH_{3(aq)} + 3H_2O_{(l)} \qquad Eq.3.5$$

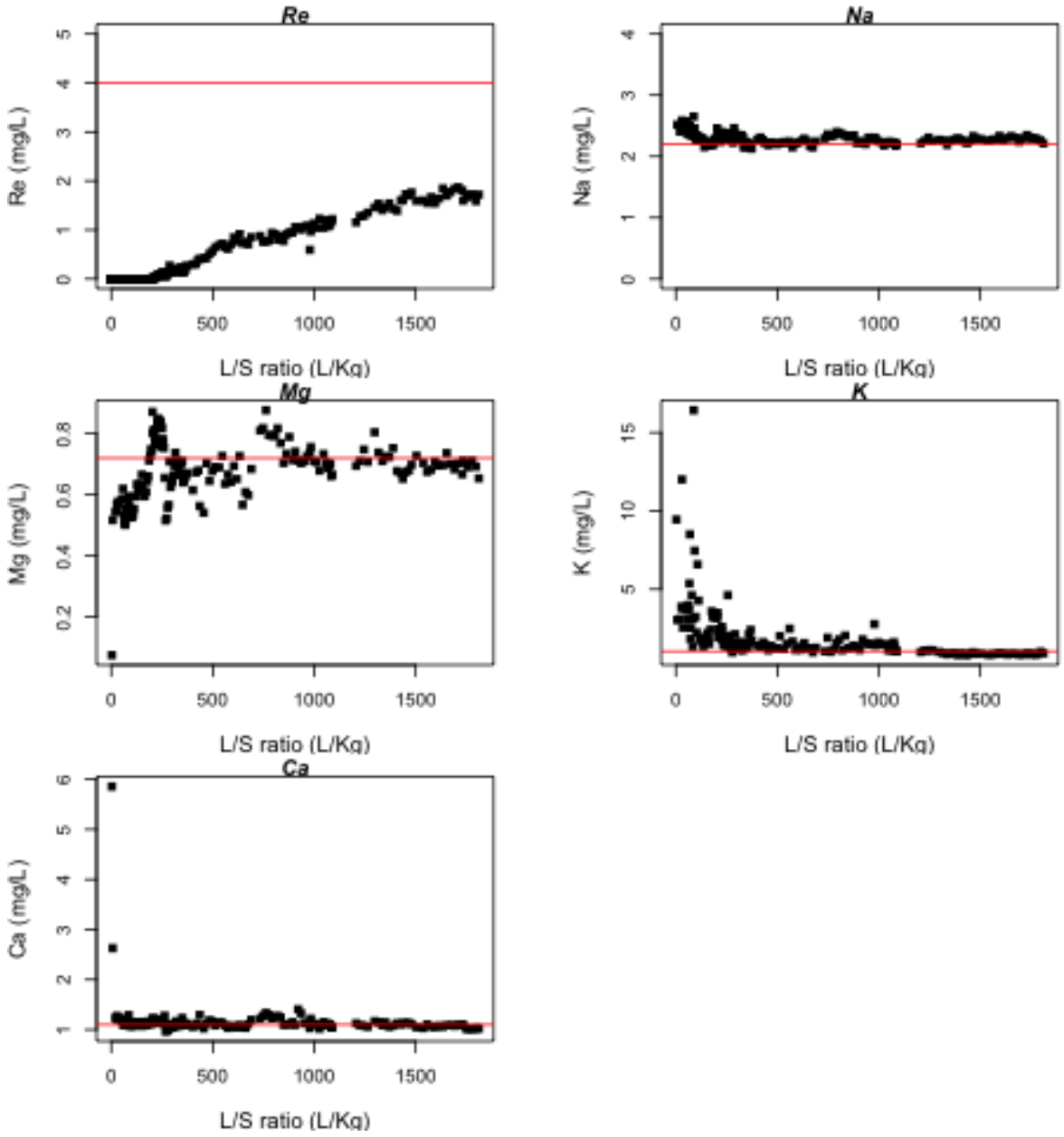


*Figure 3.5: Major elements detected in the column effluent for the Re + AGW leachate treatment, the red line represents the inlet concentration.*

The effluent leaching pattern for the major elements present in the Re + AGW leachate treatment are shown above, Figure 3.5. As discussed above, limited Re was initially detected

in the column effluent at around 250 L $Kg^{-1}$. The effluent Re concentration slowly increases to ≈ 2 mg $L^{-1}$ over the extended course of leaching until the test was ended at 1811 L $Kg^{-1}$, illustrating the high capacity for the PIC material to retain Re in the absence of competing oxidants. For the major common cations present in the AGW surrogate (i.e., Na, Mg, K and Ca), there was some initial fluctuation at the beginning of the test that may be attributed to solutes associated with the sand and PIC materials. However, the effluent concentrations for the major cations were generally consistent with the inlet solution composition.

### 3.4 Discussion

Serval important trends were demonstrated in the column tests. Very limited Re sorption was observed for the no sorbent sand control column, with essentially full Re breakthrough observed after very limited leaching. Additionally, the effluent pH remained fairly constant over the course of the test and no soluble Fe was detected. For the two $NO_3^-$ free tests, Re in NaCl and Re + AGW, Re was greatly retained in the column and significant Fe was detected in the effluent. Rhenium was only detectable after considerable leaching and never reached the inlet concentration, with somewhat greater Re retention observed in the low ionic strength AGW treatment. In the presence of $NO_3^-$, initial Re detection in the effluent occurred earlier with full breakthrough during the course of leaching, illustrating the impact of the competing oxidant. In addition, much less soluble Fe was detected in the effluent for the $NO_3^-$ containing leachate, suggesting more complete Fe oxidation associated with the higher concentration of oxidants. Limited $NO_3^-$ was initially detected in the column effluent with little to no $NO_2^-$ buildup and $NH_3$ levels that are consistent with complete $NO_3^-$ reduction. Eventually greater $NO_3^-$ breakthrough and a decrease in effluent $NH_3$ levels coincided with Re breakthrough, indicating that the available reductive capacity had been largely consumed.

# CHAPTER 4

# SUMMARY AND CONCLUSIONS

## 4.1 Summary of findings

Technetium-99 ($^{99}$Tc), one of several radioactive isotopes of technetium (Tc), is a beta emitter ($\beta^- \approx 249$ keV) with a half-life of 211,000 years that decays to form stable ruthenium-99. Technetium-99 is a nuclear fission product of uranium-235 ($^{235}$U), with a fission yield (i.e., fuel rods of uranium dioxide that contain ~3% $^{235}$U) of 6.03 % (Luykx, 1986, Hu et al., 2010). On the Department of Energy's (DOE) Savannah River Site (SRS, Aiken, SC), the processing of spent nuclear materials used in the production of plutonium (Pu) and tritium ($^3$H) has generated a large inventory of radiological waste materials containing $^{99}$Tc and other radionuclides that threaten soil and groundwater resources.

Numerous technologies have been developed and implemented for treating contaminated groundwater resources, including the widely employed pump-and-treat method, where contaminated groundwater is extracted and the contaminants of concern are removed using various conventional water treatment methods prior to eventual disposal. Such methods are quiet expensive, of limited effectiveness and require continuous management and maintenance (Mackay and Cherry, 1989, Nyer, 2000). Numerous *in situ* treatment methods have been developed as an alternative. The use of permeable reactive barriers (PRBs) provides a potentially cost effective alternative for addressing a range of groundwater contaminants (Puls et al., 1999). Contaminated groundwater passes through the PRB and the

contaminants are immobilized or transformed to a less toxic species. Since $^{99}Tc$ is redox sensitive, with the reduced Tc(IV) species being considerable less mobile than Tc(VII), an effective PRB material would facilitate Tc(VII) reduction and/or sorption in a manner that facilitates long-term immobilization. Zero-Valent Iron (ZVI) materials have been widely demonstrated to effectively immobilize and/or transform a wide range of redox sensitive contaminants (i.e., TCE, PCE, Cr(VI), U(VI), Pu, $NO_3^-$, etc.) (Cantrell et al., 1995, Ponder et al., 2000, Xin et al., 2015, Hwang et al., 2011, Qiu et al., 2012, Gu et al., 1998), and therefore reflect a potential material for the effective treatment of Tc(VII), both as an *in situ* PRB and more directly as waste-water filter material. However, previous studies have identified significant limitations to the effective use of ZVI materials for contaminant treatment.

Currently, there are several commercially available iron products that are marketed for the remediation of contaminated water. This study assessed the ability of four commercially available iron materials (a novel porous iron composite material, reagent grade Zero Valent Iron, and two Fe oxides) to immobilize rhenium (Re), as an analogue for Tc, from contaminated groundwater in the presence and absence of common oxidants, such as nitrate and dissolved oxygen, that are likely present in nuclear waste water streams and contaminated groundwater. To achieve this objective, a series of batch experiments were carried out first to determine which materials were best at immobilizing Re from contaminated water under extended, well-mixed conditions. These experiments were performed in both oxic and anoxic environments to determine the impact of $O_2$, as well as in the presence and absence of $NO_3^-$.

In the batch experiments (Chapter 2), the PIC material performed the best by completely removing the Re from the contaminated water under both oxic and anoxic conditions, and in

the presence of $NO_3^-$. The ZVI also effectively removed Re from solution at a bit slower rate when compared to the PIC. However, the ZVI was more sensitive to the presence of $NO_3^-$. In contrast, the two Fe oxide materials had limited impact on Re, with GFH1 displaying no detectable Re sorption when compared to the no sorbent control and the GFH2 sorbing ≈ 20% of the Re.

In addition to the composition of water (i.e., $NO_3^-$), the iron speciation of the solid phase (i.e., Iron oxides vs zero-valent iron) has played a prominent role in the fate of Re. In fact, the materials containing only iron oxides and/or oxy-hydroxides (i.e., GFH1 and GFH2) shows no significant immobilization effect, as opposed to the $Fe^0$ materials (i.e., PIC and ZVI). As the zero-valent iron has a strong reduction capacity, this suggest that the reduction of Re plays a significant role in reducing its mobility in solution. On the PIC materials, the newly formed $Fe_3O_4$ species may also sorb $ReO_4^-$, which can become entrapped in its structure, providing another mechanism for $ReO_4^-$ removal from the bulk solution.

In addition to the batch studies, dynamic column experiments (Chapter 3) were conducted using the PIC material under kinetically limited conditions that are more analogous to applications as a PRB or waste-water treatment filter. Four sets of extended column experiments were carried out to evaluate the removal of $^{99}Tc$, as the highly mobile oxidized pertechnetate species (i.e., $TcO_4^-$). The first using sand as a control, the second using the PIC material with a Re solution, the third used the PIC material with a Re solution containing $NO_3^-$, and the fourth using the PIC material with a Re and Artificial Groundwater (AGW) solution.

For the column experiments, it was observed that in the absence of $NO_3^-$ (Re in NaCl and Re + AGW), Re was greatly retained in the column with failure to achieve full breakthrough

after 90 L leachate. Significant $Fe_{(aq)}$ was detected in the effluent, with somewhat greater Re retention observed in the lower ionic strength AGW treatment. In the presence of $NO_3^-$, initial Re detection in the effluent occurred much earlier (0.105 L leachate), with full breakthrough observed during the course of leaching (11 L leachate), illustrating the impact of the competing oxidant. In addition, much less soluble Fe was detected in the effluent for the $NO_3^-$ containing leachate, suggesting more complete Fe oxidation associated with the higher concentration of oxidants. In addition, considerable $NO_3^-$ was reduced to form $NH_3$ despite the high effluent pH with very limited $NO_2^-$ buildup.

### 4.2 Recommendation for future research

The current study clearly demonstrates the superiority of the novel PIC material when compared to the three other Fe-based sorbents. While this study has shed light on many aspects of Tc/Re behavior in the presence of $Fe^0$, several questions remain that warrant additional study. While thermodynamic data exist for several potential Tc oxy-hydroxide reduction products, i.e., $TcO_2$-$c_{(s)}$, $TcO_2 \cdot 1.6H_2O_{(s)}$, and $Tc_2 \cdot 2H_2O_{(s)}$ (Cantrell and Williams, 2012, Cantrell et al., 2013), this is not the case for Re. In addition, a recent study by Li et al., (2018) using synchrotron-based techniques to evaluate solid phase speciation found very little evidence for Re(VII) reduction compared to Tc(VII) under similar batch conditions using both the PIC and ZVI, despite considerable sequestration of both Tc(VII) and Re(VII). As demonstrated in the current study, Li et al., (2018) found that the PIC material was more effective than the ZVI at immobilizing both Tc and Re. However, these results suggest that the reactions for Re(VII) immobilization in the $Fe^0$ system may be quite different than that of Tc(VII), despite batch evidence that ongoing Fe oxidation is required for Re(VII)

immobilization. Clearly, additional spectroscopic studies using both XAFS or XANES are warranted to better evaluate the Re-Fe systems as an analogue for Tc-Fe systems.

## REFERENCES


ABDELOUAS, A., GRAMBOW, B., FATTAHI, M., ANDRES, Y. & LECLERC-CESSAC, E. 2005. Microbial reduction of 99 Tc in organic matter-rich soils. *Science of the Total Environment,* 336**,** 255-268.

ADRIANO, D. 1986. Trace elements in the terrestrial environment Springer-Verlag. *New York***,** 219-262.

ADRIANO, D. 2001a. Trace elements in terrestrial environments: 2nd edition. Springer-Verlag. *New York.*

ADRIANO, D., WENZEL, W., VANGRONSVELD, J. & BOLAN, N. 2004. Role of assisted natural remediation in environmental cleanup. *Geoderma,* 122**,** 121-142.

ALEKSANYAN, A. Y., PODOBAEV, A. & REFORMATSKAYA, I. 2007. Steady-state anodic dissolution of iron in neutral and close-to-neutral media. *Protection of Metals,* 43**,** 66-69.

ALLRED, B. 2012. Laboratory evaluation of porous iron composite for agricultural drainage water filter treatment. *Transactions of the ASABE,* 55**,** 1683-1697.

APHA 1997a. Method-4500-$NH_3$ Nitrogen. *Standard Methods for the Examination of Water and Wastewater.* Washington , DC 20005.

APHA 1997b. Method-4500-$NO_2^-$ (Nitrogen). *Standard Methods for the Examination of Water and Wastewater.* Washington , DC 20005.

APPELO, C. A. J. & POSTMA, D. 2004. *Geochemistry, groundwater and pollution*, CRC press.

ARTINGER, R., BUCKAU, G., ZEH, P., GERAEDTS, K., VANCLUYSEN, J., MAES, A. & KIM, J.-I. 2003. Humic colloid mediated transport of tetravalent actinides and technetium. *Radiochimica Acta,* 91**,** 743-750.

BADRUZZAMAN, M., WESTERHOFF, P. & KNAPPE, D. R. 2004. Intraparticle diffusion and adsorption of arsenate onto granular ferric hydroxide (GFH). *Water Research,* 38**,** 4002-4012.

BEASLEY, T. & LORZ, H. 1986. A review of the biological and geochemical behaviour of technetium in the marine environment. *Technetium in the Environment.* Springer.

BLEAM, W. F. 2016. *Soil and environmental chemistry,* Academic Press.

BLOWES, D. W., PTACEK, C. J., BENNER, S. G., MCRAE, C. W., BENNETT, T. A. & PULS, R. W. 2000. Treatment of inorganic contaminants using permeable reactive barriers1. *Journal of Contaminant Hydrology,* 45**,** 123-137.

BOULDING, J. R. & GINN, J. 1995. Soil, Vadose zone and Ground-Water Contamination. *Assessment, Prevention, and Remediation***,** 733-739.

BROOKINS, D. G. 1986. Rhenium as analog for fissiogenic technetium: Eh-pH diagram (25°C, 1 bar) constraints. *Applied Geochemistry,* 1**,** 513-517.

BRUNO, J. & EWING, R. C. 2006. Spent Nuclear Fuel *Elements,* 2**,** 343-349.

BUCK, E. C., HANSON, B. D. & MCNAMARA, B. K. 2004. The geochemical behaviour of Tc, Np and Pu in spent nuclear fuel in an oxidizing environment. *Geological Society, London, Special Publications,* 236**,** 65-88.

CALDERON, B. & FULLANA, A. 2015. Heavy metal release due to aging effect during zero valent iron nanoparticles remediation. *Water research,* 83**,** 1-9.

CANTRELL, K. J., CARROLL, K. C., BUCK, E. C., NEINER, D. & GEISZLER, K. N. 2013. Single-pass flow-through test elucidation of weathering behavior and evaluation of contaminant release models for Hanford tank residual radioactive waste. *Applied Geochemistry,* 28**,** 119-127.

CANTRELL, K. J., KAPLAN, D. I. & WIETSMA, T. W. 1995. Zero-valent iron for the in situ remediation of selected metals in groundwater. *Journal of Hazardous Materials,* 42**,** 201-212.

CANTRELL, K. J. & WILLIAMS, B. D. 2012. Equilibrium Solubility Model for Technetium Release from Saltstone Bsed on Single-Pass Flow Eperiments. Richland, Washington: Pacific Northwest National Laboratory.

CANTRELL, K. J. & WILLIAMS, B. D. 2013. Solubility control of technetium release from Saltstone by TcO2·xH2O. *Journal of Nuclear Materials,* 437**,** 424-431.

CARNIATO, L., SCHOUPS, G., SEUNTJENS, P., VAN NOOTEN, T., SIMONS, Q. & BASTIAENS, L. 2012. Predicting longevity of iron permeable reactive barriers using multiple iron deactivation models. *Journal of Contaminant Hydrology,* 142**,** 93-108.

CHEN, A., SHANG, C., SHAO, J., ZHANG, J. & HUANG, H. 2017. The application of iron-based technologies in uranium remediation: A review. *Science of the Total Environment,* 575**,** 1291-1306.

CHENG, I. F., MUFTIKIAN, R., FERNANDO, Q. & KORTE, N. 1997. Reduction of nitrate to ammonia by zero-valent iron. *Chemosphere,* 35**,** 2689-2695.

COUGHTREY, P. J., JACKSON, D. & THORNE, M. 1983. *Radionuclide distribution and transport in terrestrial and aquatic ecosystems. A critical review of data. Volume 3,* AA Balkema.

CRANE, R. A., DICKINSON, M. & SCOTT, T. B. 2015. Nanoscale zero-valent iron particles for the remediation of plutonium and uranium contaminated solutions. *Chemical Engineering Journal,* 262**,** 319-325.

DARAB, J. G. & SMITH, P. A. 1996. Chemistry of technetium and rhenium species during low-level radioactive waste vitrification. *Chemistry of Materials,* 8**,** 1004-1021.

DAVIES, B. E. 1980. *Applied soil trace elements*, Wiley.

DE VRIES, J. J. & SIMMERS, I. 2002. Groundwater recharge: An overview of processes and challenges. *Hydrogeology Journal,* 10**,** 5-17.

DELEGARD, C. & BARNEY, G. 1983. Effects of Hanford high-level waste components on sorption of cobalt, strontium, neptunium, plutonium, and americium on Hanford sediments. Rockwell International Corp., Richland, WA (USA). Rockwell Hanford Operations.

DESMET, G. & MYTTENAERE, C. 1986. *Technetium in the Environment*, Springer Science & Business Media.

DILLON, P., RHEBERGEN, W., MILLER, M. & FALLOWFIELD, H. 2000. Groundwater: past achievements and future challenges. *Sililo et al (eds) Balkema, Rotterdam*.

DING, Q., QIAN, T., YANG, F., LIU, H., WANG, L., ZHAO, D. & ZHANG, M. 2013. Kinetics of reductive immobilization of rhenium in soil and groundwater using zero valent iron nanoparticles. *Environmental Engineering Science*, 30**,** 713-718.

DRISCOLL, F. G. 1986. Groundwater and wells. *St. Paul, Minnesota: Johnson Filtration Systems Inc., 1986, 2nd ed.,* 1.

EPA, U. S. 2002. EPA Facts about Technetium-99.

EVOQUA. 2014. *GFH Media Removes Arsenic in Arizona Water Supply* [Online]. Internet: Evoqua Water Technologies. Available: http://www.evoqua.com/en/brands/IPS/productinformationlibrary/ES-AZGFH-CS.pdf [Accessed 2018].
FARRELL, J., BOSTICK, W. D., JARABEK, R. J. & FIEDOR, J. N. 1999. Uranium removal from ground water using zero valent iron media. *Groundwater,* 37**,** 618-624.
FLURY, B., FROMMER, J., EGGENBERGER, U., MADER, U., NACHTEGAAL, M. & KRETZSCHMAR, R. 2009. Assessment of long-term performance and chromate reduction mechanisms in a field scale permeable reactive barrier. *Environmental science & technology,* 43**,** 6786-6792.
FOLLETT, R. F. & HATFIELD, J. L. 2001. Nitrogen in the environment: sources, problems, and management. *The Scientific World Journal,* 1**,** 920-926.
FOTH, H. D. 1978. Fundamentals of soil science. *Soil Science,* 125**,** 272.
FU, F., DIONYSIOU, D. D. & LIU, H. 2014. The use of zero-valent iron for groundwater remediation and wastewater treatment: A review. *Journal of Hazardous Materials,* 267**,** 194-205.
GANDHI, S., OH, B.-T., SCHNOOR, J. L. & ALVAREZ, P. J. 2002. Degradation of TCE, Cr (VI), sulfate, and nitrate mixtures by granular iron in flow-through columns under different microbial conditions. *Water Research,* 36**,** 1973-1982.
GAVASKAR, A. R., GUPTA, N., SASS, B., JANOSY, R. & OSULLIVAN, D. 1998. Permeable barriers for groundwater remediation.
GU, B., LIANG, L., DICKEY, M., YIN, X. & DAI, S. 1998. Reductive precipitation of uranium (VI) by zero-valent iron. *Environmental Science & Technology,* 32**,** 3366-3373.
GUAN, X., DONG, H., MA, J., LO, I. M. & DOU, X. 2011. Performance and mechanism of simultaneous removal of chromium and arsenate by Fe (II) from contaminated groundwater. *Separation and Purification Technology,* 80**,** 179-185.
GUAN, X., SUN, Y., QIN, H., LI, J., LO, I. M., HE, D. & DONG, H. 2015. The limitations of applying zero-valent iron technology in contaminants sequestration and the corresponding countermeasures: the development in zero-valent iron technology in the last two decades (1994–2014). W*ater Research,* 75**,** 224-248.
GUERIN, T. F., HORNER, S., MCGOVERN, T. & DAVEY, B. 2002. An application of permeable reactive barrier technology to petroleum hydrocarbon contaminated groundwater. *Water Research,* 36**,** 15-24.
HARTER, R. D. & SMITH, G. 1981. Langmuir equation and alternate methods of studying "adsorption" reactions in soils. *Chemistry in the Soil Environment***,** 167-182.
HORNBERGER, G. M., WIBERG, P. L., RAFFENSPERGER, J. P. & D'ODORICO, P. 2014. *Elements of physical hydrology*, JHU Press.
HU, B. 2011. Permeable Porous Composite. North American Hoganas.
HU, B. 2016. Permeable porous composite. Google Patents.
HU, Q.-H., WENG, J.-Q. & WANG, J.-S. 2010. Sources of anthropogenic radionuclides in the environment: a review. *Journal of Environmental Radioactivity,* 101**,** 426-437.
HU, Q., ZHAO, P., MORAN, J. E. & SEAMAN, J. C. 2005. Sorption and transport of iodine species in sediments from the Savannah River and Hanford Sites. *Journal of Contaminant Hydrology,* 78**,** 185-205.
HWANG, Y.-H., KIM, D.-G. & SHIN, H.-S. 2011. Mechanism study of nitrate reduction by nano zero valent iron. *Journal of Hazardous Materials,* 185**,** 1513-1521.

ICENHOWER, J. 2010. The biogeochemistry of technetium; a review of the behavior of an artificial element in the natural environment. *American Journal of Science (1818-1819),* 310**,** 721-752.
ISTOK, J., SENKO, J., KRUMHOLZ, L. R., WATSON, D., BOGLE, M. A., PEACOCK, A., CHANG, Y.-J. & WHITE, D. C. 2004. In situ bioreduction of technetium and uranium in a nitrate-contaminated aquifer. *Environmental Science & Technology,* 38**,** 468-475.
JIANG, Z., LV, L., ZHANG, W., DU, Q., PAN, B., YANG, L. & ZHANG, Q. 2011. Nitrate reduction using nanosized zero-valent iron supported by polystyrene resins: role of surface functional groups. *Water Research,* 45**,** 2191-2198.
JUSTE, C. 1988. Appréciation de la mobilité et de la biodisponibilité des éléments en traces du sol. *Science du sol,* 26**,** 103-112.
KABATA-PENDIAS, A. 2010. *Trace elements in soils and plants,* CRC press.
KAPLAN, D., MATTIGOD, S., PARKER, K. & IVERSEN, G. 2000. Experimental work in support of the 129I-disposal special analysis. *Westinghouse Savannah River Company, Aiken, SC. Radioiodine Biogeochemistry,* 2329.
KAPLAN, D., PARKER, K. & ORR, R. 1998. Effects of High-pH and High-Ionic-Strength Groundwater on Iodide, Pertechnetate, and Selenate Sorption to Hanford Sediments: Final Report for Subtask 3a. Pacific Northwest National Laboratory, Richland, WA.
KAPLAN, D. & SERNE, R. 1995. *Distribution coefficient values describing iodine, neptunium, selenium, technetium, and uranium sorption to Hanford sediments,* Pacific Northwest National Laboratory.
KAZMANN, R. G. 1988. *Modern Hydrology: Dedicated to the Memory of Oscar Edward Meinzer, November 28, 1876-June 14, 1948, the Father of Modern Geohydrology*, "The" National Water Well Association.
KIM, E. 2003. Chemistry of rhenium as an analogue of technetium: Experimental studies of the dissolution of rhenium oxides in aqueous solutions. *Radiochimica Acta,* 91**,** 211-216.
KIM, E. & BOULÈGUE, J. 2003. Chemistry of rhenium as an analogue of technetium: Experimental studies of the dissolution of rhenium oxides in aqueous solutions. *Radiochimica Acta,* 91**,** 211-216.
KINNIBURGH, D. G. 1986. General purpose adsorption isotherms. *Environmental Science & Technology,* 20**,** 895-904.
KLEYKAMP, H. 1985. The chemical state of the fission products in oxide fuels. *Journal of Nuclear Materials,* 131**,** 221-246.
KOVALICK, W. & KINGSCOTT, J. 1995. Progress in clean-up and technological developments in US Superfund Program. *Contaminated Soil'95.* Springer.
KUTYNAKOV, D. K. I. & PARKER, K. E. 1998. Radionuclide distribution coefficients for sediments collected from borehole 299-E17-21: Final report for subtask 1a. Pacific Northwest National Laboratory, Richland, WA.
LANGMUIR, D. 1997. *Aqueous Environmental Geochemistry*.
LANGMUIR, I. 1918. The adsorption of gases on plane surfaces of glass, mica and platinum. *Journal of the American Chemical society,* 40**,** 1361-1403.
LENELL, B. A. & ARAI, Y. 2017. Perrhenate sorption kinetics in zerovalent iron in high pH and nitrate media. *Journal of Hazardous Materials,* 321**,** 335-343.
LEO, A., HANSCH, C. & ELKINS, D. 1971. Partition coefficients and their uses. *Chemical Reviews,* 71**,** 525-616.

LI, L., BENSON, C. H. & LAWSON, E. M. 2006. Modeling porosity reductions caused by mineral fouling in continuous-wall permeable reactive barriers. *Journal of Contaminant Hydrology,* 83**,** 89-121.
LIANG, L., GU, B. & YIN, X. 1996. Removal of technetium-99 from contaminated groundwater with sorbents and reductive materials. *Separations Technology,* 6**,** 111-122.
LIANG, L., MOLINE, G. R., KAMOLPORNWIJIT, W. & WEST, O. R. 2005. Influence of hydrogeochemical processes on zero-valent iron reactive barrier performance: A field investigation. *Journal of Contaminant Hydrology,* 78**,** 291-312.
LIESER, K. 1993. Technetium in the nuclear fuel cycle, in medicine and in the environment. *Radiochimica Acta,* 63**,** 5-8.
LIU, H., QIAN, T. & ZHAO, D. 2013. Reductive immobilization of perrhenate in soil and groundwater using starch-stabilized ZVI nanoparticles. *Chinese Science Bulletin***,** 1-7.
LIU, T., RAO, P., MAK, M. S., WANG, P. & LO, I. M. 2009. Removal of co-present chromate and arsenate by zero-valent iron in groundwater with humic acid and bicarbonate. *Water Research,* 43**,** 2540-2548.
LUYKX, F. 1986. Technetium discharges into the environment. *Technetium in the Environment.* Springer.
LV, X., XU, J., JIANG, G., TANG, J. & XU, X. 2012. Highly active nanoscale zero-valent iron (nZVI)–Fe3O4 nanocomposites for the removal of chromium (VI) from aqueous solutions. *Journal of Colloid and Interface Science,* 369**,** 460-469.
MACKAY, D. M. & CHERRY, J. A. 1989. Groundwater contamination: pump-and-treat remediation. *Environmental Science & Technology,* 23**,** 630-636.
MACKENZIE, P. D., HORNEY, D. P. & SIVAVEC, T. M. 1999. Mineral precipitation and porosity losses in granular iron columns. *Journal of Hazardous Materials,* 68**,** 1-17.
MAK, M. S., RAO, P. & LO, I. M. 2009. Effects of hardness and alkalinity on the removal of arsenic (V) from humic acid-deficient and humic acid-rich groundwater by zero-valent iron. *Water Research,* 43**,** 4296-4304.
MARSHALL, T. J. 1959. *Relations between water and soil,* Commonwealth Agricultural Bureaux Farnham Royal Bucks, England.
MASET, E. R., SIDHU, S. H., FISHER, A., HEYDON, A., WORSFOLD, P. J., CARTWRIGHT, A. J. & KEITH-ROACH, M. J. 2006. Effect of organic co-contaminants on technetium and rhenium speciation and solubility under reducing conditions. *Environmental Science & Technology,* 40**,** 5472-5477.
MCBETH, J., LLOYD, J., LAW, G., LIVENS, F., BURKE, I. & MORRIS, K. 2011. Redox interactions of technetium with iron-bearing minerals. *Mineralogical Magazine,* 75**,** 2419-2430.
MEENA, A. H. & ARAI, Y. 2017. Environmental geochemistry of technetium. *Environmental Chemistry Letters,* 15**,** 241-263.
MEGGYES, T. & SIMON, F.-G. 2000. Removal of organic and inorganic pollutants from groundwater using permeable reactive barriers. *Land Contamination & Reclamation,* 8**,** 3.
MIELCZARSKI, J. A., ATENAS, G. M. & MIELCZARSKI, E. 2005. Role of iron surface oxidation layers in decomposition of azo-dye water pollutants in weak acidic solutions. *Applied Catalysis B: Environmental,* 56**,** 289-303.
MITRA, P., SARKAR, D., CHAKRABARTI, S. & DUTTA, B. K. 2011. Reduction of hexa-valent chromium with zero-valent iron: batch kinetic studies and rate model. *Chemical Engineering Journal,* 171**,** 54-60.

NEŠIĆ, S. 2007. Key issues related to modelling of internal corrosion of oil and gas pipelines–A review. *Corrosion Science,* 49**,** 4308-4338.
NOUBACTEP, C. 2008. A critical review on the process of contaminant removal in Fe0–H2O systems. *Environmental Technology,* 29**,** 909-920.
NOUBACTEP, C. 2014. Flaws in the design of Fe (0)-based filtration systems? *Chemosphere,* 117**,** 104-107.
NYER, E. K. 2000. Limitations of pump and treat remediation methods. *In Situ Treatment Technology, Second Edition.* CRC Press.
PIERCE, E. M., LUKENS, W. W., FITTS, J. P., JANTZEN, C. M. & TANG, G. 2014. Experimental determination of the speciation, partitioning, and release of perrhenate as a chemical surrogate for pertechnetate from a sodalite-bearing multiphase ceramic waste form. *Applied Geochemistry,* 42**,** 47-59.
POINEAU, F., FATTAHI, M., DEN AUWER, C., HENNIG, C. & GRAMBOW, B. 2006. Speciation of technetium and rhenium complexes by in situ XAS-electrochemistry. *Radiochimica Acta,* 94**,** 283-289.
PONDER, S. M., DARAB, J. G. & MALLOUK, T. E. 2000. Remediation of Cr (VI) and Pb (II) aqueous solutions using supported, nanoscale zero-valent iron. *Environmental Science & Technology,* 34**,** 2564-2569.
PULS, R. W., PAUL, C. J. & POWELL, R. M. 1999. The application of in situ permeable reactive (zero-valent iron) barrier technology for the remediation of chromate-contaminated groundwater: a field test. *Applied Geochemistry,* 14**,** 989-1000.
QIU, X., FANG, Z., YAN, X., GU, F. & JIANG, F. 2012. Emergency remediation of simulated chromium (VI)-polluted river by nanoscale zero-valent iron: laboratory study and numerical simulation. *Chemical Engineering Journal,* 193**,** 358-365.
R DEVELOPMENT CORE TEAM 2013. R development core team. *RA Lang Environ Stat Comput,* 55**,** 275-286.
RADCLIFFE, D. E. & ŠIMŮNEK, J. 2010. *Soil physics with HYDRUS: Modeling and applications,* CRC press Boca Raton, FL.
RIJNAARTS, H., BRUNIA, A. & VAN AALST, M. In situ bioscreens. Proceeding of the Fourth International In Situ and On-Site Bioremediation Symposium, 1997. Battelle Press Columbus, OH, 203-208.
RUHL, A. S., WEBER, A. & JEKEL, M. 2012. Influence of dissolved inorganic carbon and calcium on gas formation and accumulation in iron permeable reactive barriers. *Journal of Contaminant Hydrology,* 142**,** 22-32.
RYU, A., JEONG, S.-W., JANG, A. & CHOI, H. 2011. Reduction of highly concentrated nitrate using nanoscale zero-valent iron: effects of aggregation and catalyst on reactivity. *Applied Catalysis B: Environmental,* 105**,** 128-135.
SCHULTE, E. & SCOPPA, P. 1987. Sources and behavior of technetium in the environment. *Science of the Total Environment,* 64**,** 163-179.
SEAMAN, J. C. 2015. Effectiveness of Porous Iron Composite (PIC) Materials for Removing Radionuclides from Low Quality Groundwater: Batch and Column Test Results. North American Hoganas: Savannah River Ecology Laboratory.
SEAMAN, J. C., LI, D., DORWARD, E., COCHRAN, J., CHANG, H. S., TANDUKAR, M., COUTELOT, F. M. & KAPLAN, D. I. Immobilization of Radioactive materials using Porous Iron Composite Media. Waste Managment (WM2018), MARCH 18-27, 2018 2018 Phoenix, AZ.

SPARKS, D. L. 2003. *Environmental Soil Chemistry,* Academic press.
SPARKS, D. L. 2013. *Kinetics of Soil Chemical Processes,* Academic Press.
SPOSITO, G. 1984. *The Surface Chemistry of Soils,* Oxford University Press.
TAGAMI, K. 2003. Technetium-99 Behavior in the Terrestrial Environment. *Journal of Nuclear and Radiochemical Sciences,* 4**,** A1-A8.
TE CHOW, V. 1988. *Applied Hydrology,* Tata McGraw-Hill Education.
THIRUVENKATACHARI, R., VIGNESWARAN, S. & NAIDU, R. 2008. Permeable reactive barrier for groundwater remediation. *Journal of Industrial and Engineering Chemistry,* 14**,** 145-156.
UNDERWOOD, E. 2012. *Trace elements in human and animal nutrition,* Elsevier.
US, E. 1989. Evaluation of Groundwater Extraction Remedies. US Environmental Protection Agency Washington, DC.
USEPA 2007a. Method 6020A. *INDUCTIVELY COUPLED PLASMA-MASS SPECTROMETRY*.
USEPA 2007b. Method 6020A, Rev. 0. Inductively coupled plasma-mass spectrometry. *Test Methods for Evaluating Solid Waste, Physical/Chemical Methods (SW-846).* Washington, DC: Office of Solid Waste.
VAN LOON, L., DESMET, G. & CREMERS, A. 1986. The influence of the chemical form of technetium on its uptake by plants. *Speciation of Fission and Activation Products in the Environment.*
WANTANAPHONG, J., MOONEY, S. & BAILEY, E. 2006. Quantification of pore clogging characteristics in potential permeable reactive barrier (PRB) substrates using image analysis. *Journal of Contaminant Hydrology,* 86**,** 299-320.
WARWICK, P., ALDRIDGE, S., EVANS, N. & VINES, S. 2007. The solubility of technetium (IV) at high pH. *Radiochimica Acta,* 95**,** 709-716.
WEBER, A., RUHL, A. S. & AMOS, R. T. 2013. Investigating dominant processes in ZVI permeable reactive barriers using reactive transport modeling. *Journal of Contaminant Hydrology,* 151**,** 68-82.
WHARTON, M., ATKINS, B., CHARNOCKAB, J., LIVENS, F., PATTRICK, R. & COLLISON, D. 2000. An X-ray absorption spectroscopy study of the coprecipitation of Tc and Re with mackinawite (FeS). *Applied Geochemistry,* 15**,** 347-354.
WILKIN, R. T., PULS, R. W. & SEWELL, G. W. 2003. Long-term performance of permeable reactive barriers using zero-valent iron: Geochemical and microbiological effects. *Groundwater,* 41**,** 493-503.
XIANG, S., CHENG, W., NIE, X., DING, C., YI, F., ASIRI, A. M. & MARWANI, H. M. 2018. Zero-valent iron-aluminum for the fast and effective U (VI) removal. *Journal of the Taiwan Institute of Chemical Engineers,* 85**,** 186-192.
XIN, J., ZHENG, X., HAN, J., SHAO, H. & KOLDITZ, O. 2015. Remediation of trichloroethylene by xanthan gum-coated microscale zero valent iron (XG-mZVI) in groundwater: Effects of geochemical constituents. *Chemical Engineering Journal,* 271**,** 164-172.
XU, J., HAO, Z., XIE, C., LV, X., YANG, Y. & XU, X. 2012. Promotion effect of Fe 2+ and Fe 3 O 4 on nitrate reduction using zero-valent iron. *Desalination,* 284**,** 9-13.
YANG, L. 2000. Enhanced bioremediation of trichloroethene contaminated by a biobarrier system. *Water Science and Technology,* 42**,** 429-434.

ZHANG, X., LIN, S., CHEN, Z., MEGHARAJ, M. & NAIDU, R. 2011. Kaolinite-supported nanoscale zero-valent iron for removal of Pb2+ from aqueous solution: reactivity, characterization and mechanism. *Water Research,* 45**,** 3481-3488.

ZHANG, Y., DOUGLAS, G. B., PU, L., ZHAO, Q., TANG, Y., XU, W., LUO, B., HONG, W., CUI, L. & YE, Z. 2017. Zero-valent iron-facilitated reduction of nitrate: Chemical kinetics and reaction pathways. *Science of the Total Environment,* 598**,** 1140-1150.

ZHOU, D., LI, Y., ZHANG, Y., ZHANG, C., LI, X., CHEN, Z., HUANG, J., LI, X., FLORES, G. & KAMON, M. 2014. Column test-based optimization of the permeable reactive barrier (PRB) technique for remediating groundwater contaminated by landfill leachates. *Journal of Contaminant Hydrology,* 168**,** 1-16.

# APPENDIX A

## XRD ANALYSIS OF IRON MATERIAL

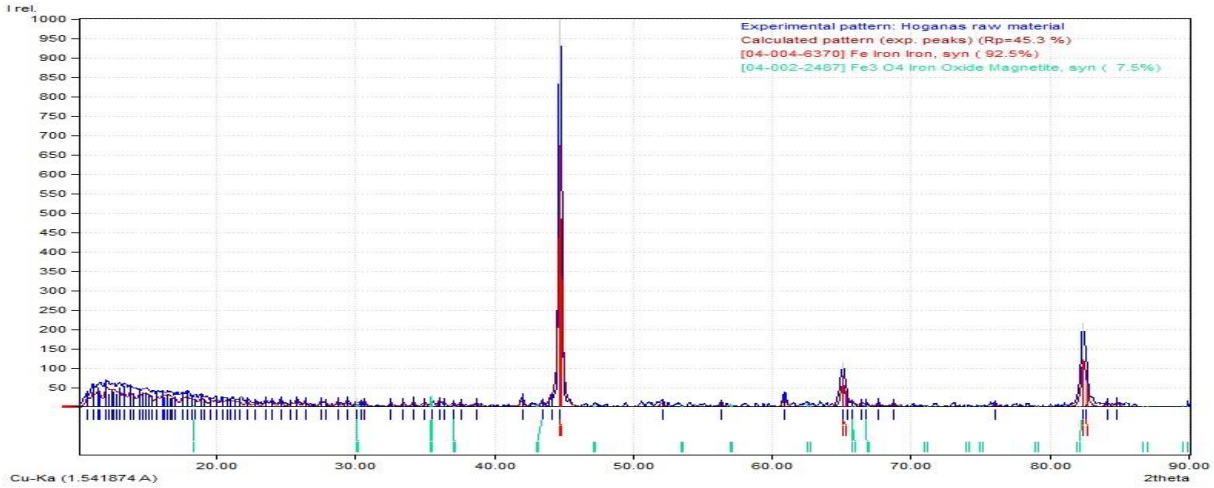


*Figure A.1: XRD analysis of the raw PIC material*

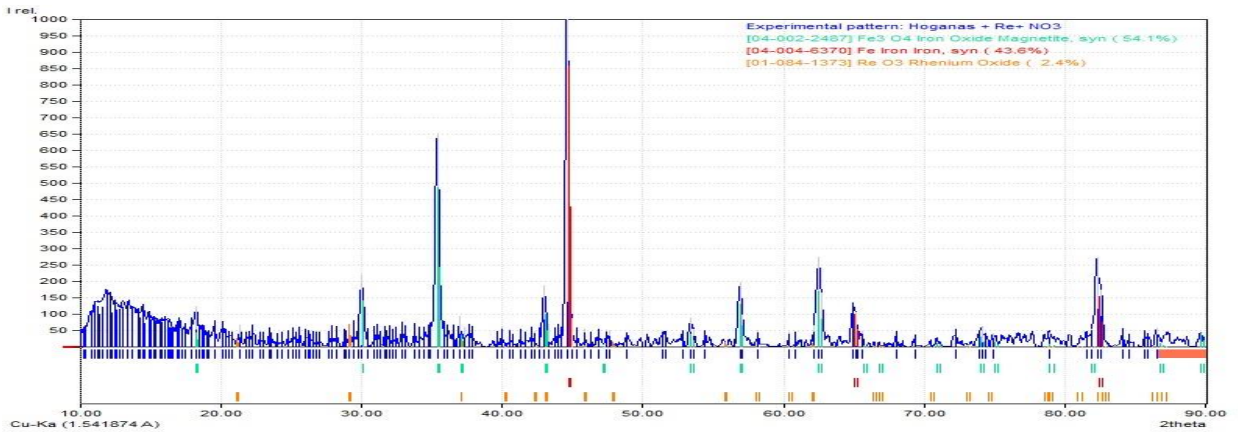


*Figure A.2: XRD analysis of the PIC material after sorption occurred with Re in the presence of* $NO_3^-$

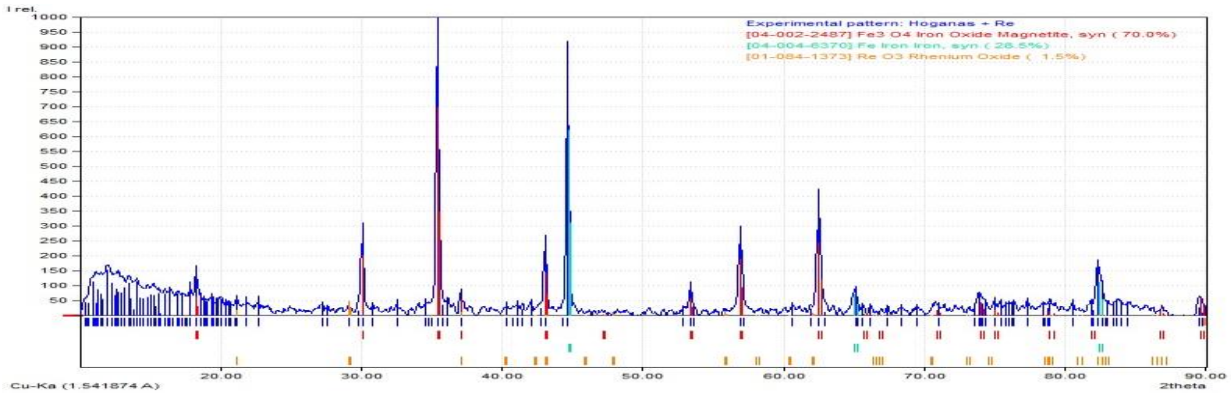


*Figure A.3: XRD analysis of the PIC material with Re*

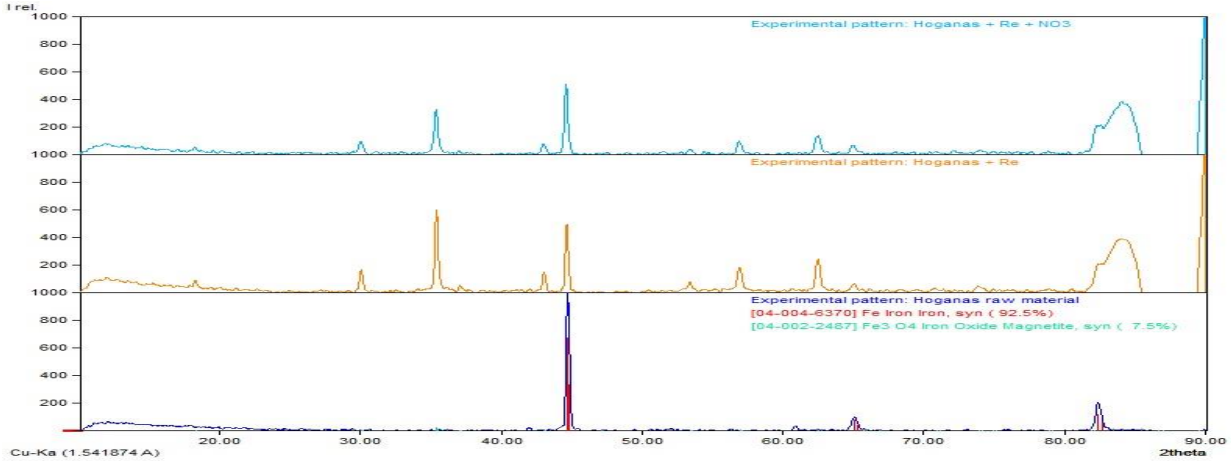


*Figure A.4: XRD analysis comparing the PIC materials*

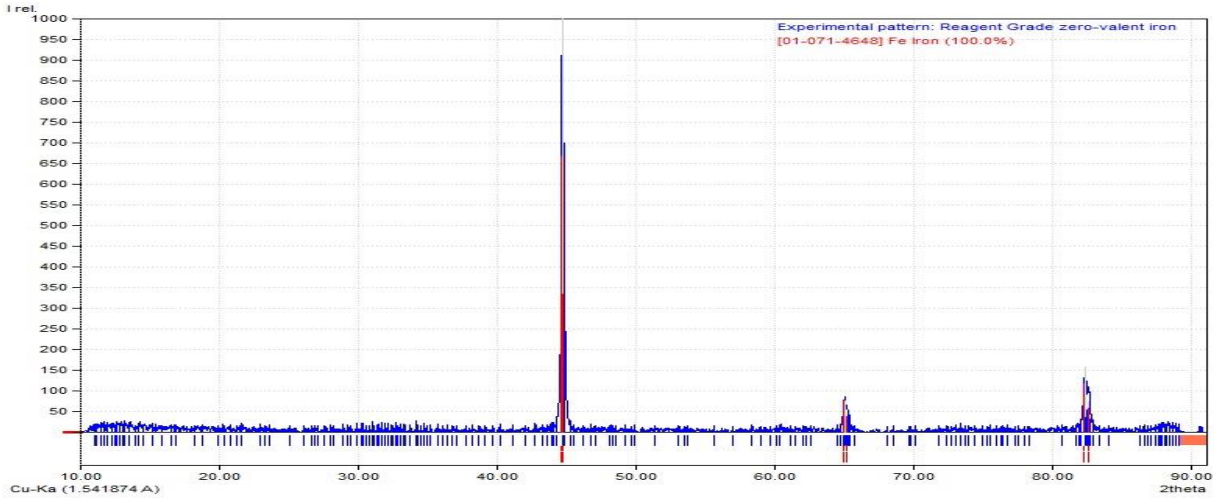


*Figure A.5: XRD analysis of the ZVI raw material*

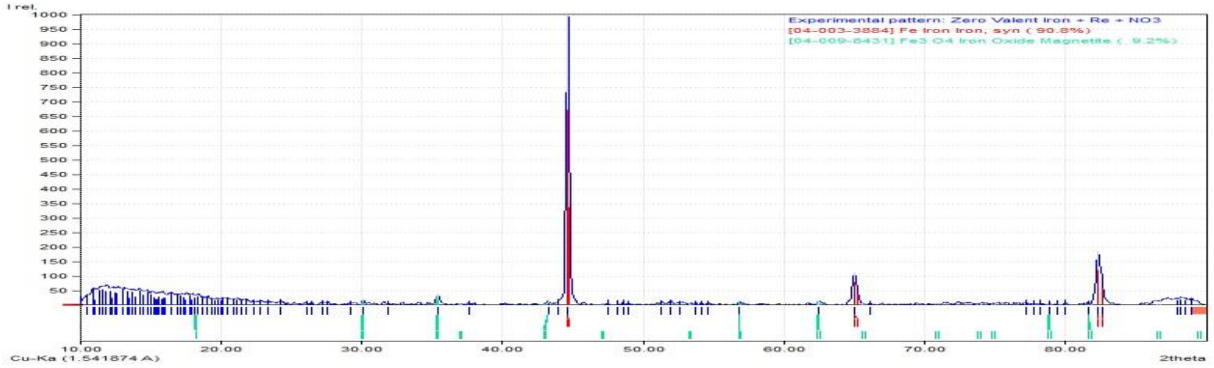


*Figure A.6: XRD analysis of the ZVI with Re in the presence of $NO_3^-$*

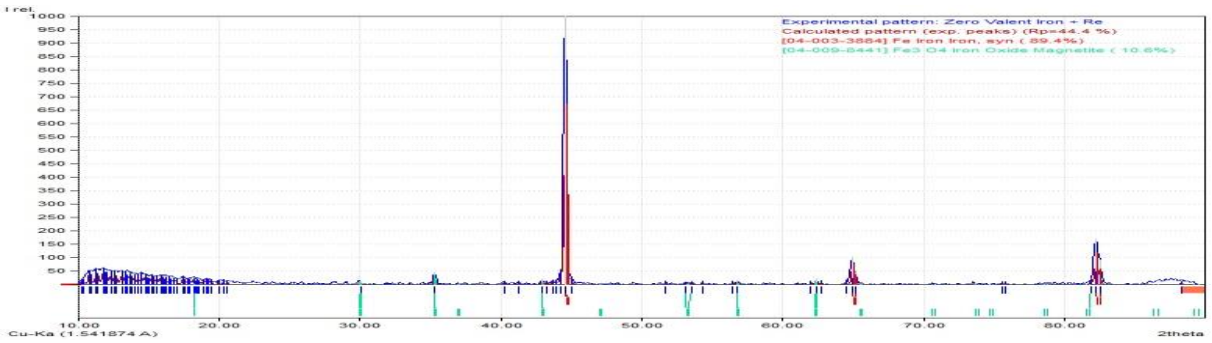


*Figure A.7: XRD analysis of the ZVI with Re*

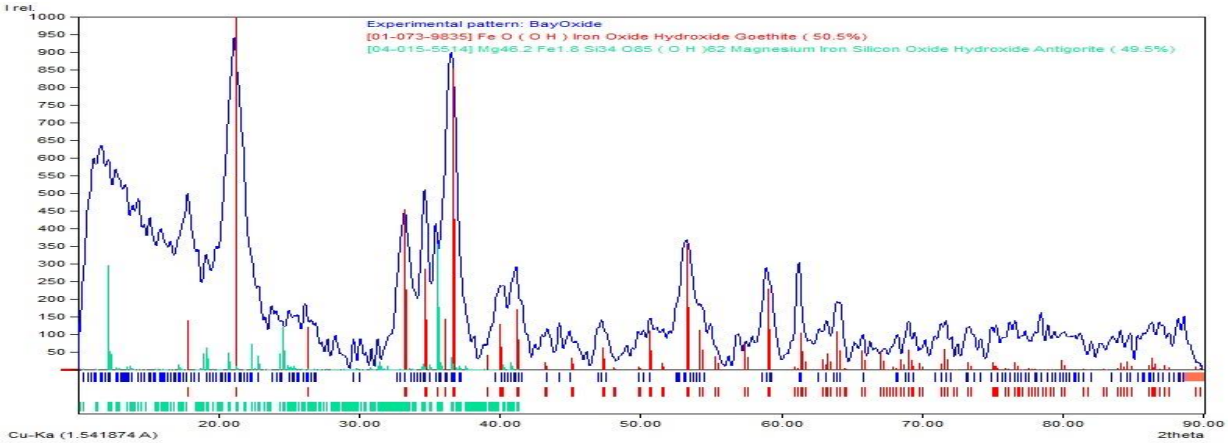


*Figure A.8: XRD analysis of the GFH1 raw material*

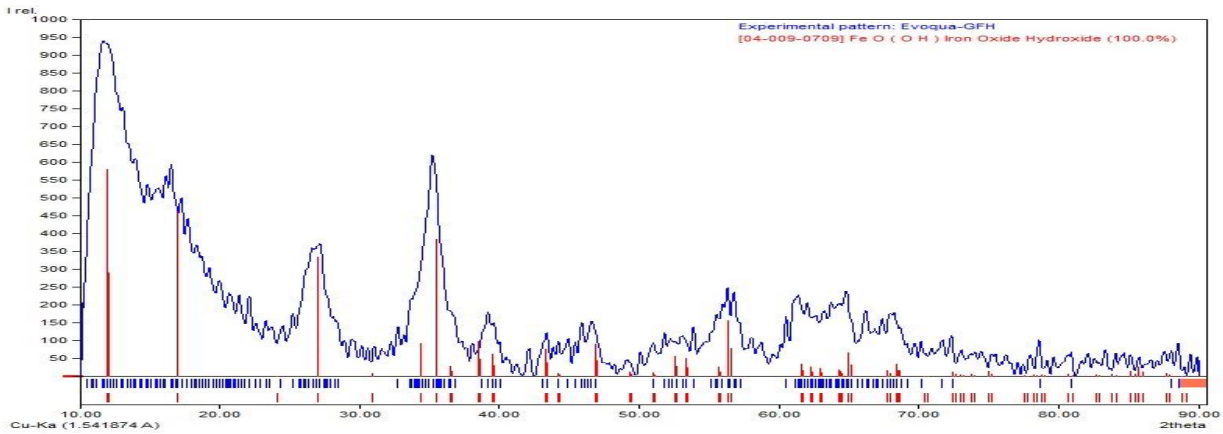


*Figure A.9: XRD analysis of the GFH2 raw material*

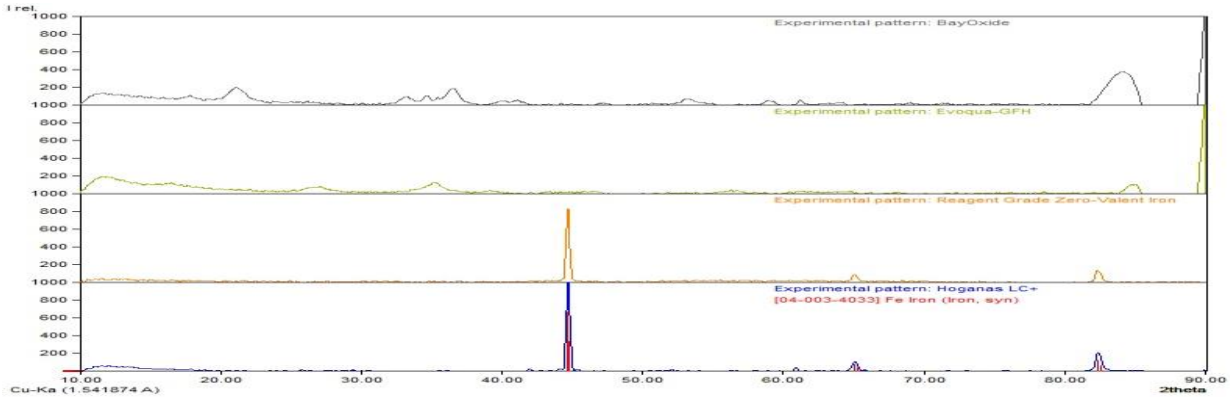


*Figure A.10: XRD analysis of each of the raw materials before sorption*